Journal of Theoretical Biology 364 (2015) 326–343

Contents lists available at ScienceDirect

Journal of Theoretical Biology

journal homepage: www.elsevier.com/locate/yjtbi

A microbial model of economic trading and comparative advantage

Peter J. Enyeart [a], Zachary B. Simpson [a,b], Andrew D. Ellington [a,b,c,*]

[a] Institute for Cell and Molecular Biology, University of Texas at Austin, Austin, TX 78712, USA
[b] Center for Systems and Synthetic Biology, University of Texas at Austin, Austin, TX 78712, USA
[c] Department of Molecular Biosciences, University of Texas at Austin, Austin, TX 78712, USA

HIGHLIGHTS

- Comparative advantage is an economic theory explaining trade interactions.
- Mathematical models of designed bacteria adhere to comparative advantage principles.
- Cooperative trading is more favored when growth is difficult to achieve.
- Self-regulated systems cooperate better at similar, lower production levels.
- Antibiotics could both attack enemies and encourage allies to cooperate.

GRAPHICAL ABSTRACT

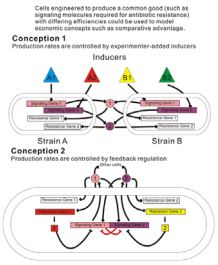

ARTICLE INFO

Article history:
Received 14 September 2013
Received in revised form
28 August 2014
Accepted 18 September 2014
Available online 28 September 2014

Keywords:
Synthetic biology
Ecology
Non-linear dynamics
Cooperation
Bacterial signaling

ABSTRACT

The economic theory of comparative advantage postulates that beneficial trading relationships can be arrived at by two self-interested entities producing the same goods as long as they have opposing relative efficiencies in producing those goods. The theory predicts that upon entering trade, in order to maximize consumption both entities will specialize in producing the good they can produce at higher efficiency, that the weaker entity will specialize more completely than the stronger entity, and that both will be able to consume more goods as a result of trade than either would be able to alone. We extend this theory to the realm of unicellular organisms by developing mathematical models of genetic circuits that allow trading of a common good (specifically, signaling molecules) required for growth in bacteria in order to demonstrate comparative advantage interactions. In Conception 1, the experimenter controls production rates via exogenous inducers, allowing exploration of the parameter space of specialization. In Conception 2, the circuits self-regulate via feedback mechanisms. Our models indicate that these genetic circuits can demonstrate comparative advantage, and that cooperation in such a manner is particularly favored under stringent external conditions and when the cost of production is not overly high. Further work could involve implementing the models in living bacteria and searching for naturally occurring cooperative relationships between bacteria that conform to the principles of comparative advantage.

1. Introduction

Comparative advantage is a mathematical concept in economics and is thought to underlie many trade interactions. The theory is usually credited to Ricardo (1817), but Torrens (1815) is also recognized as having made key insights. In simple terms, comparative advantage demonstrates that as long as two groups have differing efficiencies in producing two or more goods, it is typically to the advantage of both to engage in trade, even if one group produces all of the relevant goods with higher efficiency than the other. Though it is tempting to think of economics as a zero-sum game and assume that if one group is gaining another group must be losing, this is not necessarily the case, and comparative

* Corresponding author at: Institute for Cell and Molecular Biology, University of Texas at Austin, Austin, TX 78712, USA.
E-mail address: andy.ellington@mail.utexas.edu (A.D. Ellington).

http://dx.doi.org/10.1016/j.jtbi.2014.09.030

advantage provides a mathematical proof of this assertion. Comparative advantage has of course traditionally been applied to the study of human interactions, but the mathematical universality of the concept implies that comparative advantage could come into play anytime two self-interested entities with different resource bases come into peaceful contact with each other. For instance, two bacteria that produce and export useful metabolites at different efficiencies could find profit in trading with each other. The question then arises as to whether comparative advantage could be implemented in microbial systems.

In order to design and test such models, we must first specify what the conditions and expected results of comparative advantage are. Fortunately, comparative advantage involves specific requirements for the interacting parties and makes specific predictions about their subsequent behavior. The example that Ricardo used to illustrate the concept involves the production of wine and cloth by England and Portugal, where each has a set amount of man-hours that can be allocated toward producing either wine or cloth. Both countries are capable of producing both products, but Portugal is better at producing both than England. Specifically, Portugal can produce a greater amount of each product for the same amount of man-hours than England can. Intuition might then suggest that it is not in Portugal's interest to trade with England for either product, but this is not necessarily the case. If Portugal produces the wine it needs more efficiently than it produces cloth, and England produces the cloth it needs more efficiently than it produces wine, then cloth is more valuable to Portugal than wine, and wine is more valuable to England than cloth. It can be shown that both sides can profit by shifting resources into making the more efficient product and then trading for the other. This allows both countries individually to consume more wine and cloth through trade than either country could produce on its own. In practice, any two entities of sufficient complexity should be able to find a trading scheme that is to the advantage of both.

The requirements for demonstrating comparative advantage are therefore (1) that both countries have differing efficiencies for producing the two products, where the two have opposite relative efficiencies, and one has better absolute efficiency in producing both, and (2) that neither country can produce more of one product without producing less of the other. The specific predictions that comparative advantage makes for situations in which two such entities enter into trade are: (1) to reach maximum levels of consumption and production, both countries will specialize in manufacturing the product they make most efficiently; (2) under such conditions the amount of product available for consumption is greater for both countries than if they had not entered into trade; and (3) the country that is less efficient overall will specialize more than the more efficient country in order to balance out the higher production of the other. With this information we can begin to design microbes that might be capable of engaging in comparative advantage-like trading and formulate testable hypotheses about how they will behave.

As for how such bacteria might be designed, the tools of the burgeoning field of synthetic biology can be used to engineer bacteria to demonstrate desired behaviors. In particular, the practice of using synthetic biology to model social or ecological interactions has come to be called "synthetic ecology" (Dunham, 2007). Building on the artificial genetic oscillators (Elowitz and Leibler, 2000) and switches (Gardner et al., 2000) that formed the foundation of synthetic biology, the sub-field of synthetic ecology has thus far successfully modeled a number of social systems in microbes, including mutualist interactions between two strains trading essential nutrients (Biliouris et al., 2012; Hu et al., 2010; Kerner et al., 2012; Kubo et al., 2013; Shendure et al., 2005; Shou et al., 2007; Wintermute and Silver, 2010), predator prey relationships (Balagadde et al., 2008), and communally synchronized cyclic behavior (Danino et al., 2010; Mondragon-Palomino et al., 2011). Additionally, a great deal of work in recent years has concerned competition between cooperative producers and selfish consumers in designed microbial populations (Celiker and Gore, 2013; Chuang et al., 2009, 2010; Craig Maclean and Brandon, 2008; Datta et al., 2013; Diggle et al., 2007; Gore et al., 2009; Greig and Travisano, 2004; Nahum et al., 2011; Rainey and Rainey, 2003; Sanchez and Gore, 2013; Tanouchi et al., 2012; Waite and Shou, 2012).

Such engineered biological models occupy a useful intellectual territory between, on the one hand, mathematical and computational models, which can be criticized for being too simple to accurately represent reality or for experimenter bias in selecting parameters or other model characteristics, and, on the other, natural biological systems, which tend to be extremely complex and frequently involve confounding variables that interact in unpredictable ways with the phenomenon of interest. Synthetic biological models, on the other hand, provide the experimenter with a significant measure of control over the system's behavior but still ultimately play out in the context of actual living organisms with all their inherent complexity and unpredictability. In the present case, using comparative advantage as a model provides a framework for implementing more nuanced models of cooperation than the synthetic ecology systems that have been implemented thus far, which typically involve trade between two strains with mutually exclusive capabilities, or cases where the strains can be simply partitioned into "producers" and "cheaters."

The microbial context also provides an interesting test of the generality of comparative advantage. In particular, the systems employed by bacteria to sense and respond to their environment rely on non-linear feedback mechanisms, and direct measurements and calculations of the sort humans might employ when engaged in trade cannot be used. In the biological context, cooperation can be seen as a problem when considered in the light of basic Darwinian ideas about organisms' struggle to maximize their fitness relative to others (Hamilton, 1963). In particular, while it is clear that cooperative and altruistic actions can yield benefits to others, these actions often come at a cost to the cooperative individual, and the most obviously adaptive course is to profit from the costly cooperative behaviors of others without engaging in them oneself. In bacteria, for example, cells that have joined together into biofilms are much more difficult to eradicate than lone cells (Li and Tian, 2012). However, synthesizing and exporting the signaling molecules, extracellular polysaccharides, and the like required to coordinate a biofilm is costly, and cheaters who join biofilms without taking on these burdens often have a selective advantage (Diggle et al., 2007; Rainey and Rainey, 2003; Rumbaugh et al., 2009).

Yet clearly cooperative behaviors have been very successful throughout evolutionary history, from biopolymers to cells to multicellular organisms to human societies (Maynard Smith and Szathmáry, 1995). A variety of mathematically equivalent explanations for the success of cooperation have been provided over the last fifty years, such as kin selection (Gardner et al., 2011) and group selection (Wilson and Wilson, 2007), all based off initial work by Hamilton (1963, 1964), but one of the simpler and more general conceptualizations is that cooperative behavior can be successful whenever there is some mechanism for preferentially directing the benefits of cooperation to other cooperators, which is known as assortment (Fletcher and Doebeli, 2009).

The mechanism of assortment may be as simple as limited dispersal, where the offspring of cooperators, who are more likely to be cooperators themselves, tend not to disperse far from their parents, thus increasing the local concentration of cooperators (Diggle et al., 2007; Griffin et al., 2004; Hamilton, 1964; Kummerli et al., 2009). Cooperators may also prefer to cooperate with

genetically similar individuals, which is known as kin selection (Smith, 1964). (The definition of "kin" can also be expanded to include any suitable cooperator, thus making kin selection synonymous with assortment Gardner et al. 2011.) Conditional behaviors are another mechanism of assortment. One of the simplest and most well-studied of these is the "tit-for-tat" strategy, where cooperators choose recipients based on who cooperates in kind (Axelrod and Hamilton, 1981; Raihani and Bshary, 2011). Comparative advantage, where participants decide what and how much to give based on what they receive, is a more complex conditional behavior.

Comparative advantage can also be considered as an example of division of labor, where different participants increase their facility in one area critical for fitness at the expense of others, with the deficit made up for by differently specialized companions. Eusocial insect species provide the most well-known example of this strategy (Duarte et al., 2011; Page and Erber, 2002), but it occurs among bacteria, as well (Crespi, 2001; Shapiro, 1998), with a well-studied example being the division into nitrogen-fixing and photosynthetic cells in certain cyanobacteria (Muro-Pastor and Hess, 2012). Such cases also frequently involve complete specialization on the part of the participants, whereas comparative advantage need only deal in shifts in relative specialization (though incomplete specialization may in many cases be an evolutionary precursor to complete specialization, especially in the case of genetically identical individuals Gavrilets, 2010). Additionally, division of labor frequently involves a kin selection component, but comparative advantage has no such requirement. Thus the question of whether comparative advantage is generalizable enough to serve as a solution to the evolutionary problems faced by microbes is an interesting one.

Below we present mathematical models of both experimenter-controlled and self-regulating microbial systems designed to demonstrate comparative advantage in a bacterial system, as well as analyses of how these models perform. We find that the principles of comparative advantage do extend to these systems, and further that external stress increases the benefit gained from cooperative trading.

2. Mathematical models

2.1. Basic model

We chose to employ as a model system an extension of the one-component system used by Chuang et al. (2009, 2010) to study the interactions between "producer" bacteria, which produce and distribute necessary metabolites to the entire community, and "non-producer" bacteria, which make use of the metabolites provided by the producers but contribute nothing in return. Specifically, both bacterial strains are made to grow in the presence of antibiotics and must produce an antibiotic-resistance protein in order to reproduce. However, the gene for this protein is only expressed when a chemical signaling molecule referred to as a "quorum-sensing molecule" or "autoinducer" is present in the culture medium. This signal is manufactured by the producer strain at a certain cost to growth so that the community as a whole may grow, and the relative success of the community is assessed by measuring the growth rate (the individual strains are also tagged with different fluorescent proteins in order to allow the relative success of the two types to be measured).

To modify this system to replicate comparative advantage, we propose adding a second antibiotic along with a second antibiotic resistance gene under the control of a second signaling molecule. (However, the genes activated by the signaling molecules do not necessarily need to code for antibiotic resistance proteins, but could also code for essential amino acids or other essential molecules.) In such a system, the two signaling molecules would be the "products" traded between the two groups, and growth would be the measured output variable.

To develop a model for how such bacteria might grow, we start with the Monod (1942, 1949) equation for modeling microbial growth, which is equivalent to the Michaelis–Menten equation used in enzyme kinetics (Lehninger et al., 2013):

$$\frac{dC}{dt} = C\left[\frac{VS}{(K+S)}\right] \tag{1}$$

Here C is the density of the bacteria, S is the concentration of a substance required for growth, V is the maximum rate at which S can be converted into growth, and K is the value of S at which this rate is one half of V.

Since here we wish the bacteria to be dependent on two different products for growth, which we will call I_1 (the concentration of signaling molecule (1) and I_2 (the concentration of signaling molecule (2), we accordingly replace S in Eq. (1) with the arithmetical product of I_1I_2, which results in sigmoidal growth dynamics and reduces the growth rate to zero in the absence of either product:

$$\frac{dC}{dt} = C\left[\frac{VI_1I_2}{(K+I_1I_2)}\right] \tag{2}$$

Next we add a quantity to force the system to adhere to logistic growth, with Z as the carrying capacity. While this term is not strictly necessary since we are interested not in the final density of the cells so much as the growth rate at which that density is reached, without this term the system grows to infinity, and it is difficult to devise a consistent rule for determining the range over which the growth rate should be measured.

$$\frac{dC}{dt} = C\left[\frac{VI_1I_2}{(K+I_1I_2)}\right]\left[1-\frac{C}{Z}\right] \tag{3}$$

Finally, we add a penalty term to represent the growth deficit that results from producing the signaling molecules, which requires separate equations for the two strains, which we will call "A" and "B":

$$\frac{dC_A}{dt} = C_A\left[\frac{VI_1I_2}{(1+(I_{A1}+I_{A2})/C_AP)(K+I_1I_2)}\right]\left[1-\frac{C_A+C_B}{Z}\right] \tag{4}$$

$$\frac{dC_B}{dt} = C_B\left[\frac{VI_1I_2}{(1+(I_{B1}+I_{B2})/C_BP)(K+I_1I_2)}\right]\left[1-\frac{C_A+C_B}{Z}\right] \tag{5}$$

I_{A1} and I_{B1} here are the concentrations of signaling molecule 1 produced by strain A and strain B, respectively, and I_{A2} and I_{B2} analogously represent the amounts of signaling molecule 2 produced by the two strains, where $I_1=I_{A1}+I_{B1}$ and $I_2=I_{A2}+I_{B2}$. Since both strains should be essentially identical except in their differing production rates of the two signaling molecules, we can safely assume that the parameters V, K, P, and Z are the same for both strains.

In the penalty term $(1+(I_{N1}+I_{N2}/C_NP))$, P is analogous to the inhibition coefficient (K_I) in Michaelis–Menton kinetics (Lehninger et al., 2013) and determines the severity of the penalty, with smaller values of P leading to larger penalties. This formulation was chosen with reference to the kinetics of enzyme inhibition to penalize the strains for making more of the signaling molecules, without allowing for the possibility of negative growth (we assume bacteriostatic rather than bacteriocidal antibiotics). Since the concentration of a signaling molecule should be a linear function of the density of cells at any given time, for determining the growth penalty this concentration should be divided by the density (concentration) of cells in order to avoid penalizing the cells for the presence of other cells in addition to penalizing them

for production. (For instance, if, as a control, strains A and B are made to be identical, then the results should be the same for starting at $(C_A, C_B)=(n, n)$ and at $(C_A, C_B)=(2n, 0)$. If C_N is omitted from the denominator in the penalty term, this will not be the case.)

The penalty term could also be multiplied by K alone or by I_1I_2 alone, depending on the nature of the inhibition. However, if the inhibition affects the apparent K, then the growth inhibition will be lessened at higher values of the I_1I_2 product, which is not the behavior we would expect from such a system. Thus the growth inhibition due to producing the signaling molecules should only affect the apparent V, as in Eqs. (4) and (5) above. In other words, the situation corresponds to non-competitive inhibition in enzyme kinetics.

We note that this model is similar to one previously developed for the one-component model (Chuang et al., 2010). We increase the complexity of that model by taking into account two signaling molecules instead of one and by including a more sophisticated penalty function, and we simplify the model by not assuming a minimum growth rate.

Eqs. (4) and (5) can be considered output functions for converting production rates of the signaling molecules into measurable variables, but the key design aspects of the system come from the question of how those production rates are determined. We have devised two methods by which this might be done. In the first (Conception 1), the production rates are determined according to the concentrations of exogenous inducers added by the experimenter. In the second (Conception 2), the bacteria control the production rates themselves through feedback regulation. Conception 1 has the advantage of allowing greater control over the system and greater freedom in exploring the parameter space, while Conception 2 is more intellectually pleasing as a self-regulating system.

2.2. Model for Conception 1

In this conception, the experimenters manually control the amounts of the signaling molecules by changing the concentration of four exogenous inducers (γ_{A1}, γ_{A2}, γ_{B1}, γ_{B2}) that modulate the promoters that control expression of the genes for producing the signaling molecules I_1 and I_2 in strains A and B. This is shown schematically in Fig. 1A, and leads to the following equations for calculating the amounts of the signaling molecules:

$$I_{A1} = C_A k_{A1} \gamma_{A1} \tag{6}$$

$$I_{A2} = C_A k_{A2} \gamma_{A2} \tag{7}$$

$$I_{B1} = C_B k_{B1} \gamma_{B1} \tag{8}$$

$$I_{B2} = C_B k_{B2} \gamma_{B2} \tag{9}$$

The k_{Ni} coefficients represent the strength of the promoters regulated by the exogenous inducers and determine how effectively these inducers stimulate production of the signaling molecules. Therefore, setting these coefficients to proper values allows implementation of the necessary differences in efficiency for satisfying the requirement of comparative advantage. Eqs. (6) (through 9) could also be represented using Michaelis–Menten kinetics, but this simpler formulation can be used if functions for converting inducer concentrations into gene expression are experimentally determined so as to yield a set of inducer values that result in a linear response in the concentration of the signaling molecules.

To force the strains to make a trade-off between producing one signaling molecule or the other, we can require that $\gamma_{A1}+\gamma_{A2}=\gamma_A$ and $\gamma_{B1}+\gamma_{B2}=\gamma_B$, where γ_A and γ_B are constant

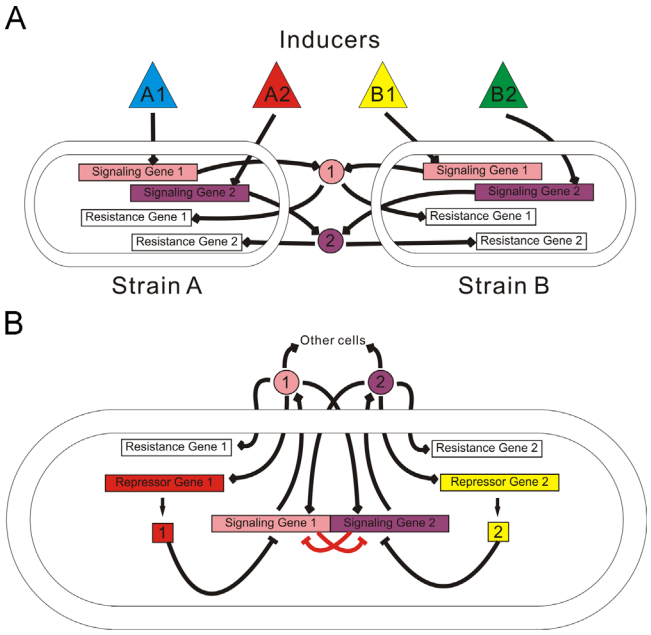

Fig. 1. Schematics of the gene circuits modeled. Circles represent signaling molecules (products), triangles represent exogenous inducers, and squares represent repressors. Pointed arrows indicate activation, and flat arrows represent inhibition. (A) Conception 1. (B) Conception 2. The black arrows represent the interactions in Conception 2.A, and the red arrows are interactions added in Conception 2.B. Note that in Conception 2 the signaling molecules are the only components that can leave to influence other cells.

for each strain and represent a resource base that the respective strains have exclusive access to. In other words, we give each strain a set amount of resources (the exogenous inducers) that can be allocated to producing one or the other signaling molecule. (For simplicity we here assume that the exogenous inducers are active over the same concentration ranges, but normalizing coefficients could be added as necessary for specific inducers.) Further, we can set "rheostat" values R_A and R_B to represent how that allocation has been made (specifically, the extent of specialization in making signaling molecule 1), where:

$$R_A = \frac{\gamma_{A1}}{\gamma_{A1}+\gamma_{A2}} = \frac{\gamma_{A1}}{\gamma_A} = 1-\frac{\gamma_{A2}}{\gamma_A} \tag{10}$$

$$R_B = \frac{\gamma_{B1}}{\gamma_{B1}+\gamma_{B2}} = \frac{\gamma_{B1}}{\gamma_B} = 1-\frac{\gamma_{B2}}{\gamma_B} \tag{11}$$

Eqs. (6) (through 9) can then be converted to:

$$I_{A1} = C_A k_{A1} \gamma_A R_A \tag{12}$$

$$I_{A2} = C_A k_{A2} \gamma_A (1-R_A) \tag{13}$$

$$I_{B1} = C_B k_{B1} \gamma_B R_B \tag{14}$$

$$I_{B2} = C_B k_{B2} \gamma_B (1-R_B) \tag{15}$$

By Combining constants such that $\kappa_{A1}=k_{A1}\ \gamma_A\ R_A$, $\kappa_{A2}=k_{A2}\ \gamma_A(1-R_A)$, $\kappa_{B1}=k_{B1}\ \gamma_B\ R_B$, and $\kappa_{B2}=k_{B2}\ \gamma_B(1-R_B)$, and then substituting into Eqs. (1) and (2), we obtain:

$$\frac{dC_A}{dt} = C_A\left[\frac{V(C_A\kappa_{A1}+C_B\kappa_{B1})(C_A\kappa_{A2}+C_B\kappa_{B2})}{(1+(\kappa_{A1}+\kappa_{A2})/P)(K+(C_A\kappa_{A1}+C_B\kappa_{B1})(C_A\kappa_{A2}+C_B\kappa_{B2}))}\right] \times\left[1-\frac{C_A+C_B}{Z}\right] \tag{16}$$

$$\frac{dC_B}{dt} = C_B\left[\frac{V(C_A\kappa_{A1}+C_B\kappa_{B1})(C_A\kappa_{A2}+C_B\kappa_{B2})}{(1+(\kappa_{B1}+\kappa_{B2})/P)(K+(C_A\kappa_{A1}+C_B\kappa_{B1})(C_A\kappa_{A2}+C_B\kappa_{B2}))}\right] \times\left[1-\frac{C_A+C_B}{Z}\right] \quad (17)$$

These equations can be non-dimensionalized to:

$$\frac{dx}{d\tau} = x\frac{(1-x-y)(\alpha x+\beta y)(\gamma x+\delta y)}{(1+\alpha+\gamma)(\epsilon+(\alpha x+\beta y)(\gamma x+\delta y))} \quad (18)$$

$$\frac{dy}{d\tau} = y\frac{(1-x-y)(\alpha x+\beta y)(\gamma x+\delta y)}{(1+\beta+\delta)(\epsilon+(\alpha x+\beta y)(\gamma x+\delta y))} \quad (19)$$

where

$$x=\frac{C_A}{Z};\quad y=\frac{C_B}{Z};\quad \tau=Vt;\quad \alpha=\frac{\kappa_{A1}}{P};\quad \beta=\frac{\kappa_{B1}}{P};\quad \gamma=\frac{\kappa_{A2}}{P};$$
$$\delta=\frac{\kappa_{B2}}{P};\quad \epsilon=\frac{K}{Z^2P^2}$$

In the non-dimensionalized equations, α, β, γ, and δ are the four parameters that determine the relative efficiencies of the two strains, while ε performs the role of K in the original equations (the other parameters fall out during the course of non-dimensionalization). Though the rheostat values R_A and R_B are not explicitly included in these equations, since they are dimensionless they could be separated out and included by replacing α, β, γ, and δ with αR_A, βR_B, $\gamma(1-R_A)$, and $\delta(1-R_B)$.

2.3. Model for Conception 2A

For Conception 2, we designed gene circuits that will allow the bacteria to make their own decisions about how to modulate signaling molecule production via feedback regulation, a very common approach in molecular systems (Lehninger et al., 2013). In the simplest scheme, each signaling molecule inhibits its own synthesis by inducing expression of a repressor that represses the gene of that signaling molecule. In order to implement a trade-off, each signaling molecule should also induce expression of the other signaling molecule. We call this implementation Conception 2A, a diagram of which is shown by the black arrows in Fig. 1B.

In a simplified mathematical model of this circuit, we can imagine each signaling molecule is produced according to Michaelis–Menten kinetics, where the signaling molecule acts as its own inhibitor, and the other signaling molecule acts as the substrate. We can therefore represent Conception 2 A with the six coupled Eqs. (20) (through 25).

$$\frac{dI_{A1}}{dt} = C_A\frac{V_{A1}(I_{A2}+I_{B2})}{k_2(1+(I_{A1}+I_{B1}/K_I))+(I_{A2}+I_{B2})} \quad (20)$$

$$\frac{dI_{A2}}{dt} = C_A\frac{V_{A2}(I_{A1}+I_{B1})}{k_1(1+(I_{A2}+I_{B2}/K_I))+(I_{A1}+I_{B1})} \quad (21)$$

$$\frac{dI_{B1}}{dt} = C_B\frac{V_{B1}(I_{A2}+I_{B2})}{k_2(1+(I_{A1}+I_{B1}/K_I))+(I_{A2}+I_{B2})} \quad (22)$$

$$\frac{dI_{B2}}{dt} = C_B\frac{V_{B2}(I_{A1}+I_{B1})}{k_1(1+(I_{A2}+I_{B2}/K_I))+(I_{A1}+I_{B1})} \quad (23)$$

$$\frac{dC_A}{dt} = C_A\left[\frac{V(I_{A1}+I_{B1})(I_{A2}+I_{B2})}{(1+(I_{A1}+I_{A2})/C_AP)(K+(I_{A1}+I_{B1})(I_{A2}+I_{B2}))}\right]\left[1-\frac{C_A+C_B}{Z}\right] \quad (24)$$

$$\frac{dC_B}{dt} = C_B\left[\frac{V(I_{A1}+I_{B1})(I_{A2}+I_{B2})}{(1+(I_{B1}+I_{B2}/C_BP))(K+(I_{A1}+I_{B1})(I_{A2}+I_{B2}))}\right]\left[1-\frac{C_A+C_B}{Z}\right] \quad (25)$$

Here V_{A1}, V_{A2}, V_{B1}, and V_{B2} represent the maximum expression rates of the genes that code for the signaling molecules and are the quantities that will be varied in order to create the conditions necessary to demonstrate comparative advantage. In an actual gene circuit, these parameters could be varied by changing the strength of the ribosome binding sites. The signaling molecules are not produced directly from the genes, of course, but are produced by enzymes that are translated from RNA molecules that are transcribed from the genes. However, this simplified model should be sufficient as an initial test of the feasibility of the system. The constants k_1 and k_2 are the concentrations of I_1 and I_2, respectively, at which expression reaches half-maximum. K_I is the inhibition constant and represents the affinity of the repressor for the operator that it binds. The inhibition term in Eqs. (20) (through 23) affects the apparent k_i in this case and not the V_{Ni}, because we expect large amounts of the substrate signaling molecule to overcome the inhibition and allow maximal expression. In terms of enzyme kinetics, this is competitive inhibition, which makes sense because the repressor and the RNA polymerase should be competing for access to the same stretch of DNA. In the actual gene circuit we would likely need at least two different k_i and two different K_I, but for theoretical purposes we assume they are all the same.

2.4. Model for Conception 2B

A potential failing of Conception 2A is that the strains do not differentiate between products made by themselves and products made by others. Specifically, in order to properly allocate resources according to the comparative advantage model, each cell must decrease the production of one signaling molecule in response to increased production by itself of the other, yet simultaneously increase production of the first signaling molecule in response to increased production by other strains of the other signaling molecule. Intracellular RNA-based inhibition mechanisms (Isaacs et al., 2004; Lucks et al., 2011; Na et al., 2013; Saito and Inoue, 2009) could be used to allow a cell to respond separately to the amount of signaling molecule it produces as opposed to the total amount of signaling molecule present. We call this modification Conception 2B, which is shown schematically by both the black and red arrows in Fig. 1B, and is implemented mathematically by replacing Eqs. (20) (through 23) with Eqs. (26) (through 29):

$$\frac{dI_{A1}}{dt} = C_A\frac{V_{A1}(I_{A2}+I_{B2})}{k_2(1+(I_{A1}+I_{B1})/K_I)(1+I_{A2}/K_{Iint})+(I_{A2}+I_{B2})} \quad (26)$$

$$\frac{dI_{A2}}{dt} = C_A\frac{V_{A2}(I_{A1}+I_{B1})}{k_1(1+(I_{A2}+I_{B2})/K_I)(1+I_{A1}/K_{Iint})+(I_{A1}+I_{B1})} \quad (27)$$

$$\frac{dI_{B1}}{dt} = C_B\frac{V_{B1}(I_{A2}+I_{B2})}{k_2(1+(I_{A1}+I_{B1})/K_I)(1+I_{B2}/K_{Iint})+(I_{A2}+I_{B2})} \quad (28)$$

$$\frac{dI_{B2}}{dt} = C_B\frac{V_{B2}(I_{A1}+I_{B1})}{k_1(1+(I_{A2}+I_{B2})/K_I)(1+I_{B1}/K_{Iint})+(I_{A1}+I_{B1})} \quad (29)$$

Here we add an extra inhibition term, $(1+(I_{Ni}/K_{Iint}))$, as a simplified model of RNA-based inhibition that serves to reduce production of one signaling molecule in response to increased production of the other in the same strain, where K_{Iint} serves as the inhibition coefficient. In actual bacteria, RNA levels could be measured by reverse transcription and quantitative PCR.

2.5. Implementation

For analysis, the equations derived above were integrated in Matlab. Integration was started from $(C_A, C_B)=(1, 1)$ (alternatively, (0, 1) or (1, 0) for monoculture controls) and, in Conception 2, $I_{A1}=I_{A2}=I_{B1}=I_{B2}=1$. Integration was then continued for 5 arbitrary

time units for each parameter set in Conception 1, and for 100 arbitrary time units for each parameter set in Conceptions 2A and 2B (Conception 1 being much more computationally intensive than Conception 2). Parameters whose values are not specified elsewhere were set to one.

Growth rate was defined as the fraction of increase per unit time from the start of growth until reaching half the carrying capacity defined by the Z parameter (i.e., if the start point is C_0, half carrying capacity is $C_{0.5}$, and the time between is t, the growth rate equals $(C_{0.5}/C_0)^{1/t}-1$). Since values at exactly half the carrying capacity ($C_{0.5}$) could not be directly obtained without using extremely resource-intensive integration parameters, we instead used the values for the growth of strains A and B (C_A and C_B) at the time points before and after the moment when C_A+C_B reached the threshold value $C_{0.5}$ to estimate the time $t_{0.5}$ required to reach $C_{0.5}$, and then used $t_{0.5}$ to estimate the values of C_A and C_B (and, in Conception 2, I_{A1}, I_{A2}, I_{B1}, and I_{B2}) when $C_{0.5}$ was reached. R^2 values for both linear and $\log_2$-linear fits of the data points in the vicinity of $C_{0.5}$ were >0.99, indicating that either could be used to provide accurate estimations of values at the point of reaching $C_{0.5}$. The results of simple linear estimation proved to be more robust to variations in the stiffness of integration, however, and so we employed the linear method. Specifically, using the subscript α to denote integrated values obtained at the point just before reaching $C_{0.5}$ and using the subscript β to denote values obtained just after reaching $C_{0.5}$, $t_{0.5}=t_\alpha+(C_{0.5}-C_\alpha)(t_\beta-t_\alpha)/(C_\beta-C_\alpha)$, and the value of any other variable x at $t_{0.5}$ is then calculated as $x_{0.5}=x_\alpha+(t_{0.5}-t_\alpha)(x_\beta-x_\alpha)/(t_\beta-t_\alpha)$.

The primary scripts used to generate the data presented are included as **Scripts 1** through **9** in the Supplemental materials online.

3. Results

3.1. Conception 1: Analysis of non-dimensionalized equations

We analyzed the non-dimensionalized Eqs. (18) and (19) in order make initial checks as to whether the model is behaving as expected. In these equations, "x" can be considered analogous to the population of strain A, and "y" can be considered as the population of strain B. Isoclines (lines along which one of the variables is fixed) occur at $x=0$ and $y=0$. The intersection between the two isoclines at (0, 0) is a fixed point, where neither variable changes. Another region where neither variable changes is along the fixed line defined by $y=1-x$. The presence of a fixed line makes sense because, if we consider the fixed-line steady-state as equivalent to the system at carrying capacity (where $x+y=1$), we do not expect the system to reach any particular value (x, y), but we do expect the ratio between x and y at the steady state to depend on the ratio between x and y at the starting point.

A flow field showing the direction and magnitude of flux at various points in the x–y plane is plotted in Fig. 2A, in which the (0, 0) fixed point appears to be an unstable node, and the fixed line appears to be stable. This is consistent with any non-zero concentration of cells growing toward carrying capacity. A phase portrait showing trajectories over time from various starting points is plotted in Fig. 2B, which again is consistent with all non-zero, non-negative starting points moving eventually onto the fixed line (reaching carrying capacity) and then stopping. Thus in these respects the model is behaving as expected.

3.2. Conception 1: Example growth curves

We performed further investigations of Conception 1 using Eqs. (16) and (17), since the variables and constants therein are more easily interpretable in biological terms. Fig. 3A shows an example of growth curves for strains A and B under conditions potentially compatible with comparative advantage (specifically, $k_{A1}=2$, $k_{A2}=1.5$, $k_{B1}=0.5$, $k_{B2}=1$, meaning that strain A makes product 1 more efficiently that product 2, strain B makes product 2 more efficiently than product 1, and strain A makes both products more efficiently that strain B). The expected sigmoidal growth curve is seen for both strains. Strain B grows faster than strain A, which is also in line with expectations since strain B produces less and thus receives a lesser growth penalty. Both rheostat values R_A and R_B are set to 0.5 in this example, which means both strains specialize equally in both products (signaling molecules), and differences in production result entirely from the differences in the values for k_{A1}, k_{A2}, k_{B1}, and k_{B2}. (R_A and R_B vary between zero and one and represent the extent to which strain A and strain B, respectively, have specialized in making product (signaling molecule) 1 as opposed to product 2.) Fig. 3B and C, which show the amounts of products 1 and 2, respectively, being produced at each time point indicate that, as expected, the highest level of production under these circumstances is strain A's production of product 1, followed by strain A's production of product 2, then strain B's production of product 2, and finally the lowest production is for strain B and product 1.

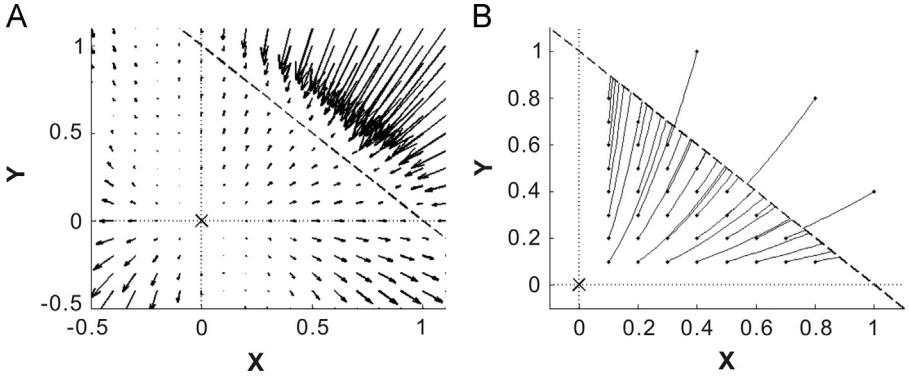

Fig. 2. Graphical analysis of the non-dimensionalized Eqs. (18) and (19) of Conception 1. The non-dimensional variables "x" and "y" correspond to cell counts or concentrations of the two different strains in the dimensional equations. Isoclines (which in this case also correspond to the x and y axes) are solid lines, the fixed line is a dotted line, and the fixed point is given by an X. The triangular region enclosed by the lines is the biologically relevant region of the parameter space. The parameter values used were $\alpha=2$, $\beta=0.5$, $\gamma=1.5$, $\delta=1$, and $\varepsilon=1$, which represent values that could potentially recreate comparative-advantage-like dynamics. (A) Phase plane analysis of the system, where each arrow is a vector representing the direction and magnitude of flow in the system at the point at which the arrow starts. (B) Phase portrait of the system, where the black lines plot trajectories in the system from various starting points denoted by black dots.

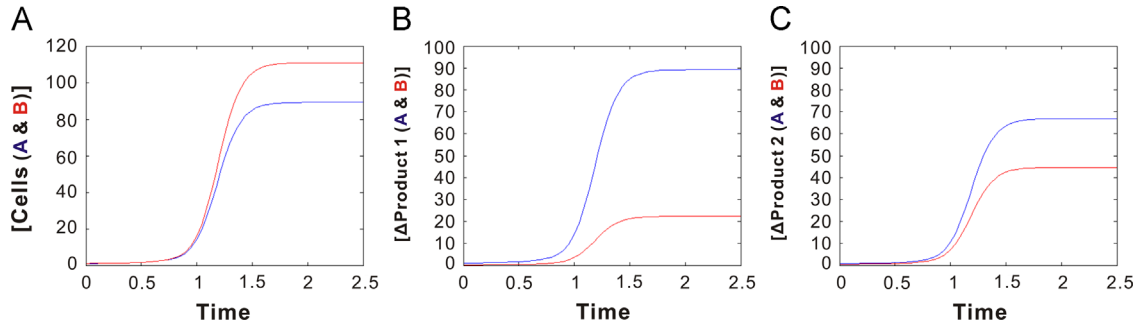

Fig. 3. Example growth curves for Conception 1. Parameter values are $K=20$, $P=20$, $V=10$, $Z=200$, $k_{A1}=2$, $k_{A2}=1.5$, $k_{B1}=0.5$, $k_{B2}=1$, and $(R_A, R_B)=(0.5, 0.5)$. Values for strain A are shown in blue, and values for strain B are shown in red. Units are arbitrary. (A) Cumulative cell concentration over time starting from a value of 1 for both strains. (B) The amount of product 1 (I_1) being produced by each strain at each time point. (C) The amount of product 2 (I_2) being produced by each strain at each time point. (For interpretation of the references to color in this figure legend, the reader is referred to the web version of this article.)

3.3. Conception 1: Investigations into the (R_A, R_B) parameter space

In order to examine the effects of different concentrations of inducers, which correspond to different degrees of specialization between the two strains, we created heat maps examining the growth rate of the system at every combination of the rheostat values R_A and R_B in increments of 0.005. Examples of such heat maps are shown in Fig. 4, and relevant output values are given in Table 1.

We first examined the dynamics of two strains with identical efficiencies allowed to specialize separately, as shown in Fig. 4A through C. There are two equivalent optimal (R_A,R_B) points. Strain A grows better when specialized to produce less than Strain B, and vice versa. Thus it is in the interest of both strains to produce less and have the other produce more. This diametrical opposition is graphically illustrated by the difference between Fig. 4B and C, which show the specialization preferences for maximal growth of each individual strain. In ecological terms, we could say that both strains are attempting to occupy the same niche, which means that at least one has to take up a suboptimal position.

Next we looked at strains designed to replicate comparative advantage. In this and all subsequent cases, strain A is the high-level producer, and strain B is the low-level producer. Fig. 4D through F show heat maps of these strains at three different levels of the parameter K. We chose to examine K because it represents the amount of difficulty the strains face in converting the products to growth and as such can likely be modulated by changing environmental factors such as the concentration of antibiotics. It is also the only parameter of out of K, P, V, and Z that still remained in some form after non-dimensionalization (as ε in Eqs. (18) and (19)), supporting the idea that it is in some sense the most important of these parameters. Increasing K from 5 to 20 (compare Fig. 4D and E) narrows the parameter space in which high growth can occur. The high-growth parameter space expands again somewhat at $K=80$ (Fig. 4F), though we note that the area representing the lowest growth rates (the area of the darkest color) is greater, as well. The values in Table 1 also show that increasing K reduces growth rates, as expected.

We also note that the degrees of specialization occurring at the optimal (R_A,R_B) are in line with expectations: both strains are specializing in the product they make more efficiently, and strain B is completely or almost completely specialized, as can be seen from the optimal (R_A,R_B) values given for the comparative advantage cases in Table 1. We also note that changing K does not seem to significantly change the optimal (R_A,R_B). Only the combined-growth heat maps are shown for these cases because the heat maps of the individual preferences did not look much different, which would seem to indicate that the interests of the two strains are now aligned. In ecological terms, they can now occupy different niches, and cooperation now becomes more advantageous.

In Fig. 4G through I we examine the effects of changing the efficiencies between the two strains. Fig. 4G and H represent cases where the efficiencies of strain A or B are reversed with respect to the case in Fig. 4E. This results in a state of absolute advantage, where strain A still makes both products more efficiently than strain B, but now both have similar relative efficiencies. The growth rates are lower than for the comparative advantage case shown in Fig. 4E (see Table 1), as expected, and furthermore, the optimal (R_A,R_B) involves strain A specializing in the product it makes less efficiently, most likely because strain B is unable to take up the slack if strain A specializes in its preferred product. A case in which the efficiencies of both strain A and strain B are reversed with respect to Fig. 4E is shown in Fig. 4I, which as expected successfully recapitulates the specialization and improved growth characteristics of comparative advantage.

We further note that strain B consistently grows better than strain A, which is a result of its lower production and therefore lower growth penalty. Thus strain A and strain B can be considered partly analogous to the producer and non-producer strains examined by Chuang et al. (2009, 2010); alternatively, the work of Chuang and coworkers can be considered as a limit case for the system presented here.

3.4. Conception 1: Effects of varying K, P, and V

Next we examined in more detail the effects on the system of varying K, P, and V. As mentioned above, K represents the degree of difficulty with which the strains convert products into growth and can likely be externally modulated by changing the antibiotic concentration. The parameter P represents the growth penalty for generating product, with small values of P corresponding to a greater penalty. The P parameter is likely intrinsic to the system and not easily modified. The parameter V represents the maximum rate with which the products can be converted into growth. The V parameter could likely be modified by changing the strength of the promoters regulating the antibiotic resistance genes activated by the products.

The effects on growth of varying these three parameters are explored in Fig. 5. Increasing K decreases overall growth rates (first row, first column of Fig. 5), as expected, and also generally increases the benefit to cooperation as judged by the ratios of coculture versus monoculture growth rates for the two strains (second row, first column of Fig. 5), where apparent thresholds exist which when crossed significantly increase the benefit to coculture, which then levels off. Increasing K also narrows the growth advantage of strain B (third row, first column of Fig. 5) perhaps because as growth becomes harder to achieve, the penalty

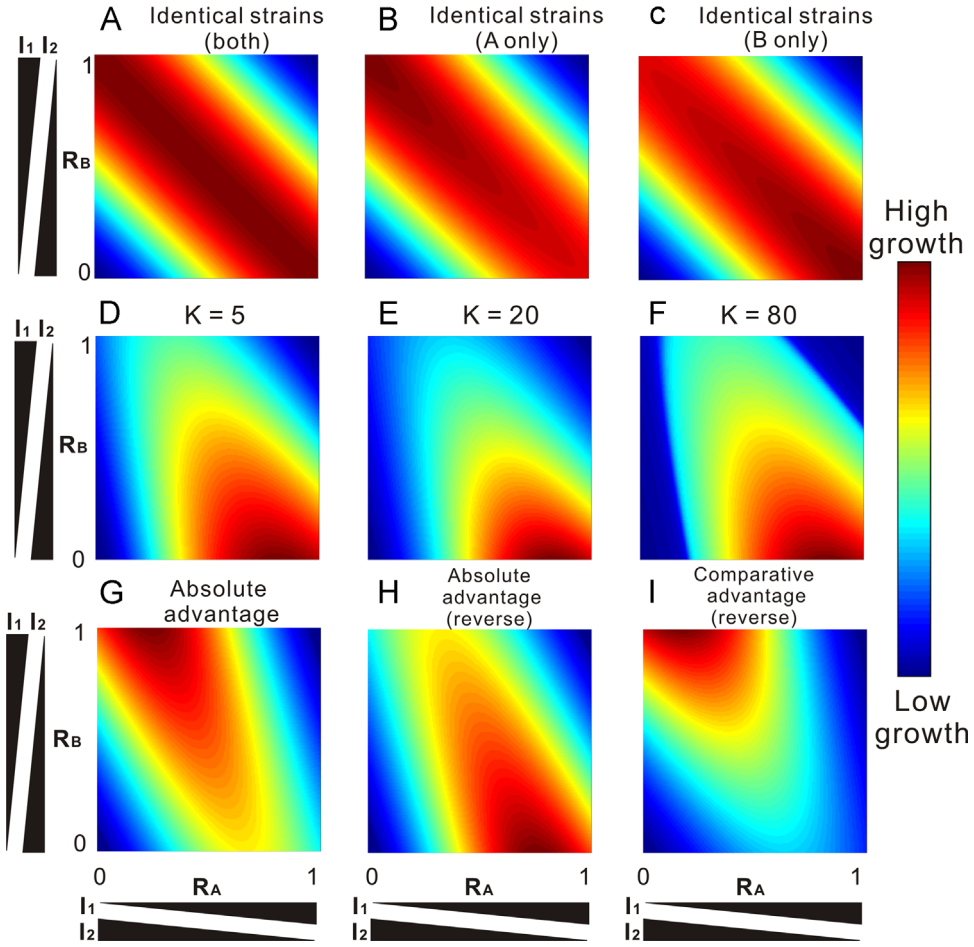

Fig. 4. Heat maps for representative parameter sets in Conception 1. The *x*-axis is R_A (the specialization of strain A in making product 1 versus product 2), the *y*-axis is R_B (the specialization of strain B in making product 1 versus product 2), and color represents relative growth rate. Default parameter values are $K=20$, $P=20$, $V=10$, $Z=200$, $k_{A1}=2$, $k_{A2}=1.5$, $k_{B1}=0.5$, $k_{B2}=1$, which are conditions that should result in behavior consistent with comparative advantage. (A) through (C) represent a control case where two identical strains are permitted to specialize differently, such that $k_{A1}=k_{B1}=2$ and $k_{A2}=k_{B2}=1.5$. (A) depicts overall growth rates, (B) depicts the growth rates of strain A, and (C) depicts the growth rates of strain B. The optimal (R_A,R_B) for (B) and the optimal (R_A,R_B) for (C) are equivalent and together represent the optimal (R_A,R_B) for (A). (D) through (F) represent different values for K in the comparative advantage context. Specifically, $K=5$ in (D), 20 in (E), and 80 in (F). (G) through (I) show variations on the efficiencies of production between strains. Specifically, $k_{A1}=2$, $k_{A2}=1.5$, $k_{B1}=1$, $k_{B2}=0.5$ (absolute advantage control) in (G), $k_{A1}=1.5$, $k_{A2}=2$, $k_{B1}=0.5$, $k_{B2}=1$ (absolute advantage control with reversed specializations) in (H), and $k_{A1}=1.5$, $k_{A1}=k_{A2}=2$, $k_{B1}=1$, $k_{B2}=0.5$ (comparative advantage positive control with reversed specializations) in (I).

Table 1
Output values for the heat maps in Fig. 4.

Relevant figure	Optimal (R_A,R_B)	Overall growth rate at optimal (R_A,R_B)	Growth rate of strain A at optimal (R_A,R_B)	Growth rate of strain B at optimal (R_A,R_B)
4A through 4C (Identical strains)	(0, 0.995) and (0.995, 0)	89.1	93.8 and 84.5	93.8 and 84.5
4D ($K=5$)	(0.82, 0)	524	456	595
4E ($K=20$)	(0.835, 0)	45.5	41.7	49.3
4F ($K=80$)	(0.835, 0)	3.51	3.36	3.65
4G (Absolute advantage $k_{B1}=1$, $k_{B2}=0.5$)	(0.24, 1)	30.4	28.8	31.9
4H (Absolute advantage $k_{A1}=1.5$, $k_{A2}=2$)	(0.76, 0)	30.4	28.8	31.9
4I (Comparative advantage—reverse)	(0.165, 1)	45.5	41.7	49.3

for producing more products carries less weight compared to the benefit for successfully achieving growth.

Increasing P (second column in Fig. 5) improves growth (both absolute growth and growth in coculture relative to monoculture) up to a point and then stops, which is in line with expectations, as the penalty term in Eqs. (1) and (2) goes to one as P goes to infinity, removing its effect. Increasing P also narrows the gap between the strains, for the same reasons.

Increasing V increases growth rate (first and second rows, third column in Fig. 5), of course, and significantly widens the gap in growth rates between strain A and B (third row, third column in Fig. 5), likely because higher V makes strain B less dependent on

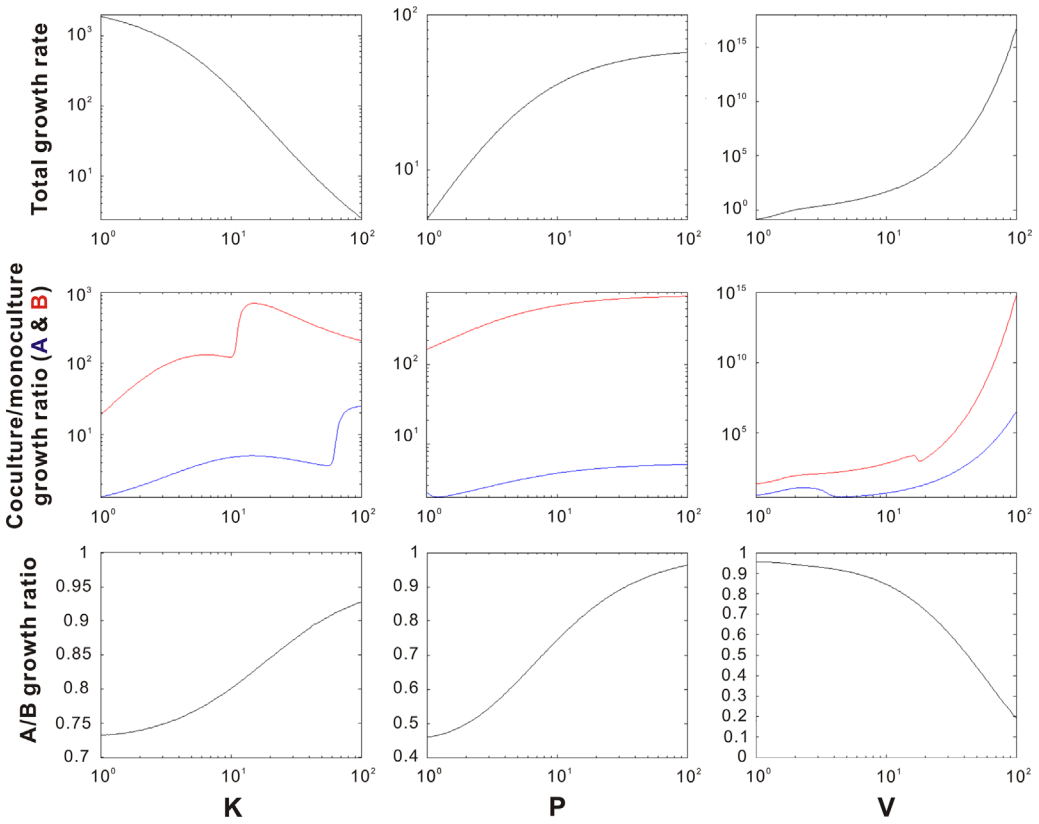

Fig. 5. Effect of *K*, *P*, and *V* parameters on growth characteristics at the optimal (R_A,R_B) in Conception 1. In all cases the *x*-axis represents the parameter value, and the *y*-axis is the resultant growth (absolute or relative). $K=20$, $P=20$, $V=10$, $Z=200$, $k_{A1}=2$, $k_{A2}=1.5$, $k_{B1}=0.5$, $k_{B2}=1$, except when a specified parameter is being varied. The first column of graphs shows the effects of varying *K*, the second column shows the effects of varying *P*, and the third column shows the effects of varying *V*. The first row shows the effect of parameter changes on the combined growth rate of strains A and B. The second row shows the effect of parameter changes on the ratio of the coculture and monoculture growth rates of the two strains, with values specific to strain A in blue, and values specific to strain B in red. The last row shows the effect of parameter changes on the ratio of the coculture growth rates of strain A and strain B. (For interpretation of the references to color in this figure legend, the reader is referred to the web version of this article.)

strain A for growth. Note also that the benefit to cooperation is consistently higher for strain B than for strain A (second row in Fig. 5). Threshold effects as seen for the *K* parameter also seem to occur with changing *V* (second row, third column in Fig. 5).

The effects of varying *K*, *P*, and *V* on specialization are shown in Movies 1, 2, and 3, respectively, which show how the heat map changes as these parameters are varied over the same ranges as in Fig. 5. The movies are available online. Increasing *K* generally either narrows the range of the high-growth parameter space or expands the range of the low-growth parameter space, which is not an unsurprising result of more difficult growth conditions. Increasing *P* initially somewhat narrows the high-growth parameter space but ceases to have much effect at higher values. As *V* increases the high-growth parameter space narrows between $V=1$ and $V=1.5$, increases from approximately $V=1.5$ to $V=3$, and thereafter decreases. In a somewhat similar fashion to *P*, changing *V* seems to have the most effect on the specialization landscape when *V* is small; when *V* is big the options narrow, perhaps as a result of accentuating the advantage gained by finding the optimal level of specialization. The optimal (R_A,R_B) (the reddest area in the heat maps) experiences little change in location as these parameters change, indicating the robustness of the specialization effect. (Also note that heat map intensities are normalized by frame, and the reddest area with one parameter set does not necessarily correspond in absolute growth rate to the reddest area with another parameter set.)

Conception 1 thus demonstrates comparative advantage. Specifically, the optimal growth conditions are those under which both strains specialize in the product they make more efficiently, with the weaker strain specializing more. Under these conditions, both strains grow better together than alone, and also grow better than under comparable absolute advantage conditions.

3.5. Conception 2: Example growth curves

Fig. 6A shows examples of growth curves for strains A and B in both Conceptions 2A and 2B under conditions potentially compatible with comparative advantage. (Conceptions 2A and 2B both involve self-regulating gene circuits, where Conception 2B contains an additional "rheostat" mechanism for forcing an intracellular trade-off in production between the two products, as shown in Fig. 1B.) The curves are similar to those seen for Conception 1 in Fig. 3A, with Conception 2B resulting in slower growth than Conception 2A, and a narrower gap between strains A and B. As seen in Fig. 6B and C, which show production levels of products 1 and 2, respectively, in a fashion analogous to Fig. 3B and C, product levels are lower yet better balanced in Conception 2B than in Conception 2A.

3.6. Conception 2: Effects of varying K, P, and V

We next repeated the analyses from Fig. 5 using the equations for Conceptions 2A and 2B. These results are shown in Fig. 7. In most cases the effects are similar, but some differences exist. Perhaps most important is the fact that, as opposed to Conception 1, coculture is not more advantageous than monoculture over the entire parameter space, particularly for strain A. In other words, cooperation between the two strains is only beneficial to both under certain conditions.

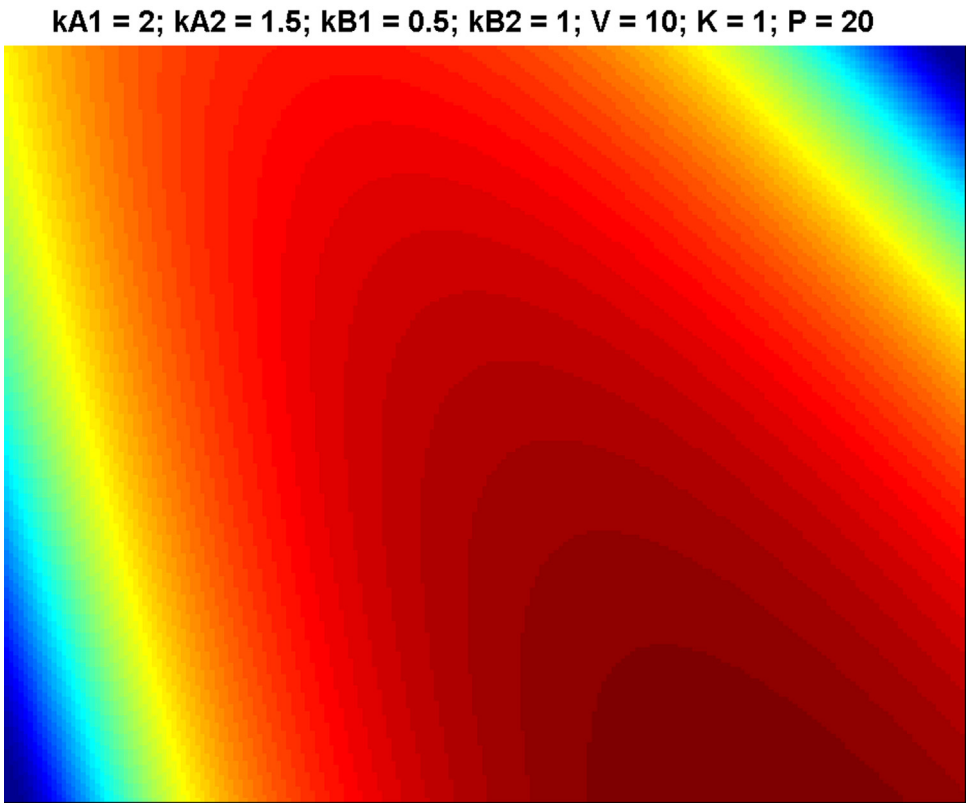

Movie 1. Effect of changing K on the specialization landscape. The x-axis is R_A, and the y-axis is R_B, with darker red representing higher growth and darker blue representing lower growth, as described in the text and **Fig. 3**. A video clip is available online. Supplementary material related to this article can be found online at http://dx.doi.org/10.1016/j.jtbi.2014.09.030.

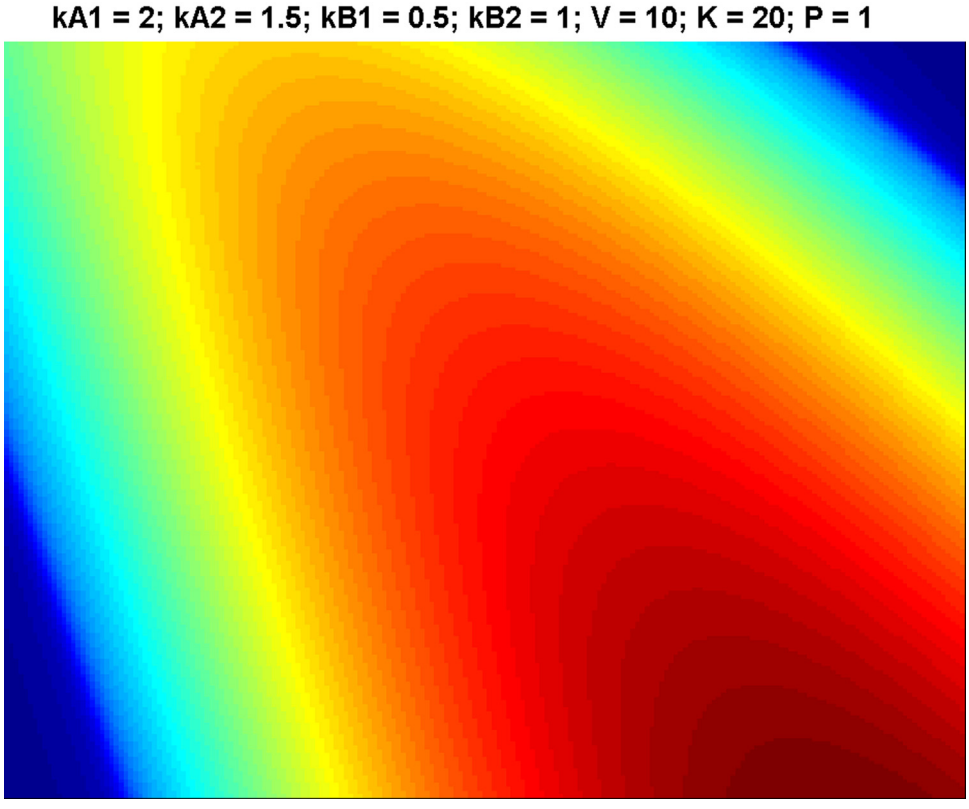

Movie 2. Effect of changing P on the specialization landscape. The x-axis is R_A, and the y-axis is R_B, with darker red representing higher growth and darker blue representing lower growth, as described in the text and **Fig. 3**. A video clip is available online. Supplementary material related to this article can be found online at http://dx.doi.org/10.1016/j.jtbi.2014.09.030.

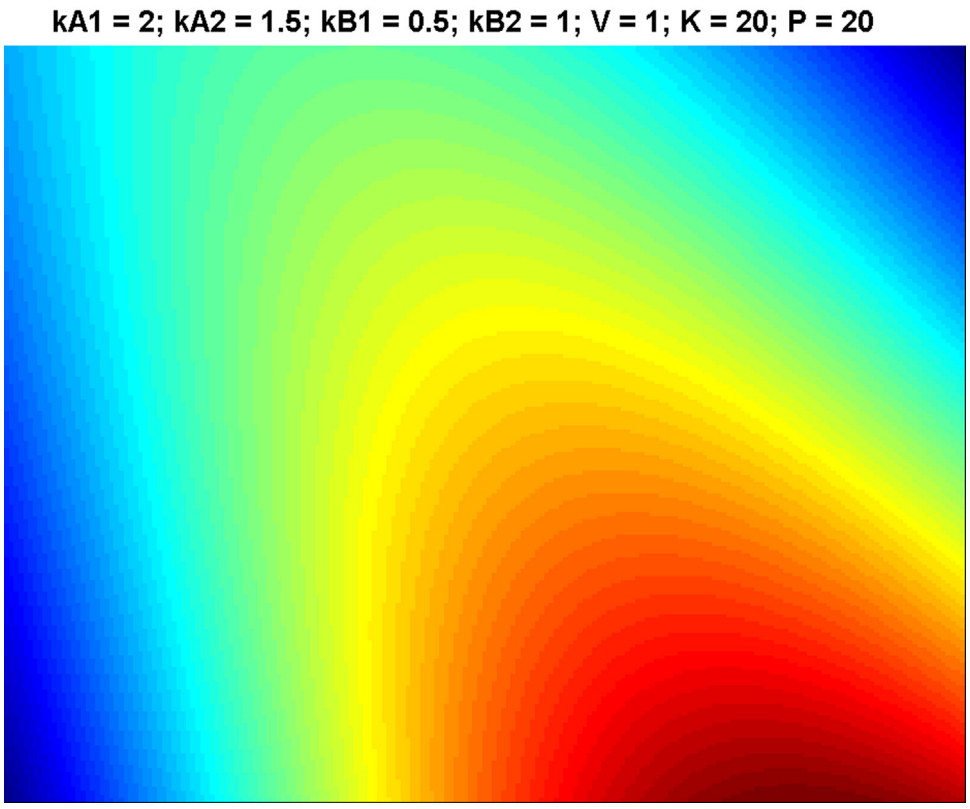

Movie 3. Effect of changing V on the specialization landscape. The x-axis is R_A, and the y-axis is R_B, with darker red representing higher growth and darker blue representing lower growth, as described in the text and **Fig. 3**. A video clip is available online. Supplementary material related to this article can be found online at http://dx.doi.org/10.1016/j.jtbi.2014.09.030.

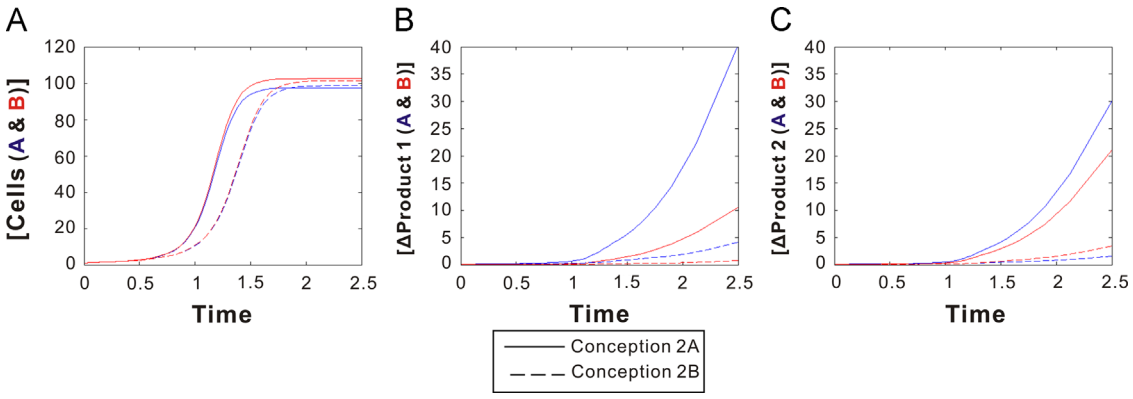

Fig. 6. Example growth curves for Conception 2. Parameter values are $K=20$, $P=20$, $V=10$, $Z=200$, $V_{A1}=2$, $V_{A2}=1.5$, $V_{B1}=0.5$, $V_{B2}=1$, which are conditions that should be compatible with comparative advantage. Otherwise the format is identical to Fig. 3, with (A) showing cumulative cell concentration, (B) showing the change in production of product 1, and (C) showing the change in production of product 2.

Specifically, coculture is advantageous for Strain A when K is above 55 for Conception 2A or above 18 for Conception 2B; when P is above 10 for Conception 2B (and never for Conception 2A when P is between 1 and 100); and when V is less than 11 for Conception 2B (and never for Conception 2A when V is between 1 and 100). (When not being varied, the parameters here are $K=20$, $P=20$, and $V=10$.)

Thus besides being interesting as a self-regulating system, Conception 2 is also interesting in providing more stringent conditions under which comparative advantage can work. In light of the discussion above, these conditions would seem to be a relatively light growth penalty for production (high P) combined with otherwise difficult growth conditions (high K and low V). In other words, capable individuals in trying circumstances benefit from cooperation, but in comfortable environments may be better off alone.

The V parameter affecting the maximum growth rate is interesting in that increasing it is beneficial for strain B but has the reverse effect on strain A, perhaps because the penalty term makes higher overall production rates more advantageous to lower-producing strain. On the other hand, Conception 2B, which adds an internal rheostat, results in increased benefit to cooperation for strain A but not for strain B, as well as lower absolute growth rates, perhaps because the internal rheostat makes it more difficult for strain B to allocate production to its less efficient (and less growth-penalizing) product, thus preventing

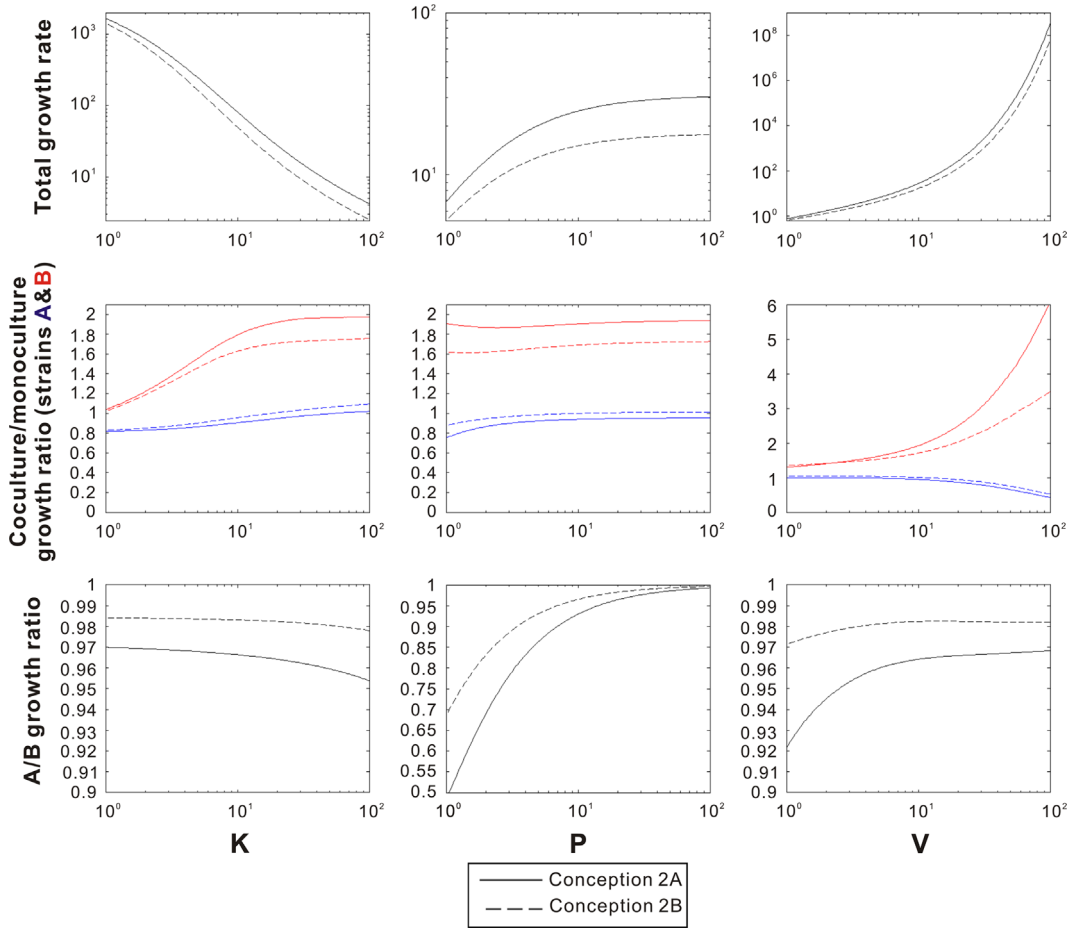

Fig. 7. Effect of *K*, *P*, and *V* parameters on growth characteristics in Conception 2. Non-varied parameter values are as in Fig. 6. Data for Conception 2A is always a solid line, while data from Conception 2B is always a dotted line. Otherwise the format is identical to Fig. 5.

it from gaining benefits from strain A without providing benefits in return.

Another interesting difference between Conceptions 1 and 2 is that in Conception 2, increasing *K* slightly reduces the ratio of the growth rates between strains A and B (third row, first column in Fig. 7), perhaps because of a combination of the less precise method for finding the optimal specialization values in Conception 2 and the fact that as *K* increases, the fraction of total production assumed by strain A increases slightly, which also increases its growth penalty. Also note that the A/B growth ratio is more robust to changing parameters in Conception 2B than in 2A (third row in Fig. 7).

3.7. Conception 2: Investigating specialization

Next we examined the extent of specialization in the strains of Conception 2 by comparing the production ratios of the two products for each strain when grown together and separately, across the same parameter variations as were studied in Fig. 7. These results are shown in Fig. 8.

Fig. 8 shows that in nearly all cases specialization is greater (i.e., the production ratios are farther from one) in coculture than in monoculture, and also that specialization is usually greater in Conception 2B than in Conception 2A, consistent with the better relative performance of Conception 2B in coculture versus monoculture. Strain B also usually specializes more than Strain A, as expected in comparative advantage, though the difference is not always large. Also interesting is that changing the parameters *K*, *P*, and *V* has little effect on specialization in monoculture but much more noticeable effects on specialization in coculture. Specialization is particularly responsive to changing parameter values in Conception 2B. Increasing *K* serves to increase specialization in the higher efficiency and higher penalty product, consistent with adversity requiring greater effort, while increasing *P* or *V* serves to decrease specialization, consistent with permissive conditions allowing laxity.

3.8. Conception 2: Further investigation of the K–P–V parameter space

To examine more fully the effects of changing the parameters *K*, *P*, and *V*, we made heat maps depicting changes in the benefit to coculture and the degree of specialization for both strains A and B across the *K*–*P*, *K*–*V*, and *P*–*V* planes in Conception 2B. We chose to focus on Conception 2B since, as discussed previously, it better adhered to the expectations of comparative advantage over a larger parameter space and was more responsive to changing parameters. The results are shown in Fig. 9. The results are consistent with those shown in Figs. 7 and 8 in that coculture is favored at high *K* and high *P*, with strain A benefitting more from coculture at low *V* and strain B benefitting more at high *V*. Specialization, on the other hand, is highest at high *K*, low *P*, and low *V* for both strains, as seen previously.

The relative influence of the different parameters can also be assessed from such heat maps, in that when a banding pattern is seen across a particular axis, the value represented by that axis can be considered to have a stronger effect on the characteristic depicted than the value on the other axis. By this reasoning, we can judge that *K* and *V* have a similar degree of influence over the

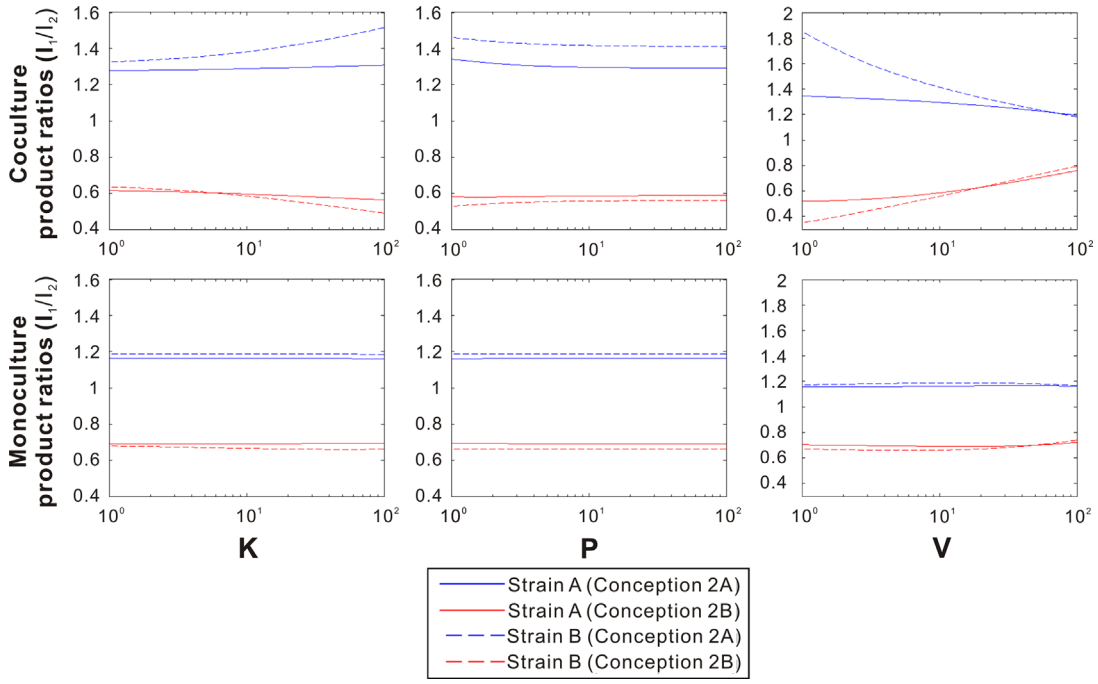

Fig. 8. Specialization in Conception 2. In all cases the *x*-axis represents the parameter value, and the *y*-axis is the production ratio of product 1 to product 2. Blue represents strain A, and red represents strain B. Results from Conception 2A are solid lines, and results from Conception 2B are dotted lines. Non-varied parameter values are as in Fig. 6. The first column of graphs shows the effects of varying *K*, the second column shows the effects of varying *P*, and the third column shows the effects of varying *V*. The first row displays results for coculture of strains A and B, and the second row displays results for monoculture. (For interpretation of the references to color in this figure legend, the reader is referred to the web version of this article.)

growth benefit from coculture, and both have much more influence than *P*. In specialization, *V* has the strongest effect, followed by *K*, and then *P*. These trends are also consistent with the data presented in Figs. 7 and 8.

3.9. Conception 2: Alternate efficiency regimes

Next we wanted to compare the previous comparative advantage cases to a case of absolute advantage differing only in that the efficiencies of strain B are swapped. These results are shown over a range of values for *K* in the first two rows in Fig. 10. (All the data in Fig. 10 is from Conception 2B, but equivalent results were obtained for Conception 2A, with trends in coculture growth benefit and specialization relative to Conception 2B similar to those in Figs. 7 and 8.) Specifically, the first row in Fig. 10 shows that the strains in the comparative advantage case gain a consistently higher benefit from cooperation than those in the absolute advantage case, and the second row in Fig. 10 shows that strain A specializes less in the absolute advantage case, while strain B specializes somewhat more and in the opposite direction from the comparative advantage case. Interestingly, this is the reverse of the absolute advantage effect seen in Conception 1 (see Fig. 4G and H), where strain A specialized in its less efficient product. The difference in effect in Conception 2 may result from each strain's ability to influence the other through its own production.

Finally, in order to examine more closely the factors that determine whether cooperation is beneficial, particularly for strain A, we looked at varying the production efficiency of strain A. Specifically, we examined the differences in coculture benefit for strain A and strain B for three different value sets: $V_{A1}=1.5$ and $V_{A2}=1.2$ (weaker strain A), $V_{A1}=2$ and $V_{A2}=1.5$ (standard strain A), and $V_{A1}=4$ and $V_{A2}=3$ (stronger strain A) over a range of *K* values. The results are shown in the third row of Fig. 10, which shows that the benefit to strain A of coculture decreases as its production strength increases, while the opposite trend is seen for strain B, which gains more from cooperation when strain A has higher production strength. Thus it seems that the stronger strain A is in comparison to strain B, the more of the burden of production it takes on.

Thus we have shown that a self-regulating microbial genetic circuit can in theory demonstrate the principles of comparative advantage, particularly when a strict trade-off in production is enforced, in adverse conditions, when the penalty for production is not too large, and when the difference in advantage between the two systems is not overly great.

4. Discussion

We have shown that comparative advantage can in principle be implemented using simple signaling and feedback systems similar to those found in bacteria, which significantly broadens the demonstrated reach of the theory. Specifically, under the right conditions in both Conception 1, where the production levels are controlled by the experimenter, and Conception 2, which employs self-regulating genetic circuits, both strains grew better together than separately and specialized in the product they could generate more efficiently, with the weaker strain specializing more completely than the stronger strain.

One interesting difference that arose in this model versus traditional models of comparative advantage is the variability in when and to what extent cooperation is beneficial to both parties in the comparative advantage context. Traditional models of comparative advantage assume that the total amount of effort expended by a given party remains constant, regardless of the amount produced. This is difficult to implement in a microbial system using current tools, and so we designed the system in terms analogous to having a relatively constant amount of raw materials, where greater or lesser effort can then be expended to produce greater or lesser amounts of products from those raw materials. This complicates the system in that the benefit to trade must be weighed against the disadvantages of increasing production. This difference results from including the penalty term and is

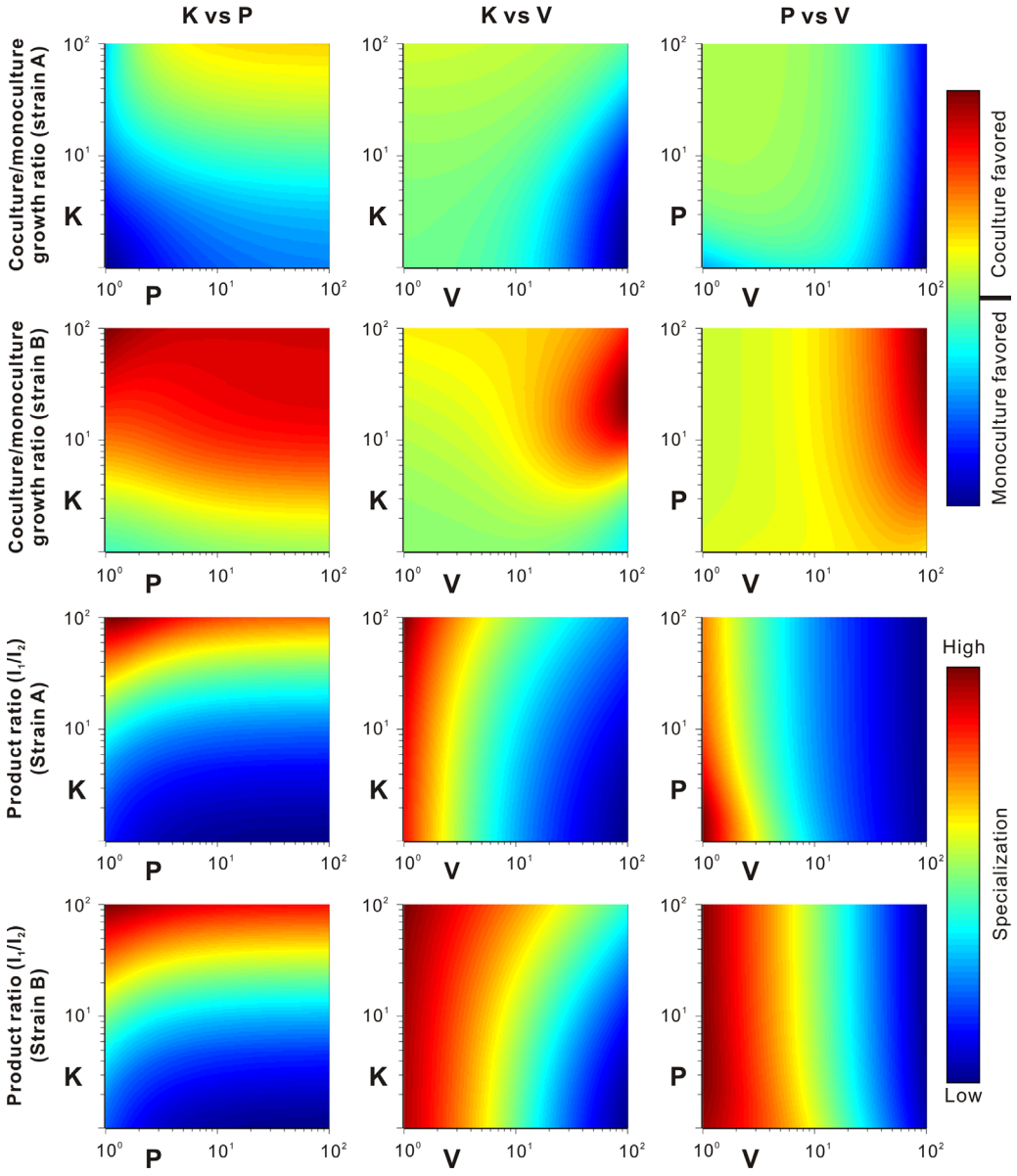

Fig. 9. Exploration of the *K*–*P*–*V* parameter space in Conception 2B. The first and second rows display the relative coculture/monoculture growth ratios for strains A and B, respectively, normalized such that a ratio of 1 is the median value on the color scale. The third and fourth rows display relative I_1/I_2 production ratios for strains A and B, respectively, where the color represents the absolute value of I_1/I_2-1. Non-varied parameter values are as in Fig. 6.

responsible for much of the surprising behavior of these models. Situations such as this, where differential resource access is relatively constant but the effort that may be required to make use of those resources is variable, also have relevance to human economic systems, and thus these results may also have applicability beyond microbial genetics. For instance, if two countries of similar size both have arable land of comparable productivity per unit area, but one country has a greater amount of arable land than the other, the country with more farmland can produce more food, but only upon investing more effort.

The most interesting property emerging from the use of the penalty term is a general trend of more stringent conditions increasing the benefit to cooperation. In particular, increasing the difficulty with which the products can be converted into growth (the *K* parameter), which can be considered at least partly a result of environmental effects, is generally associated with increased benefit to cooperation. In the current system this effect could likely be modulated by changing the antibiotic concentration. Hu and coworkers have in fact demonstrated that increased antibiotic concentration (below lethal limits) increases the benefit to cooperation in a simpler version of the system analyzed here, where each strain produces a single signaling molecule that the other needs to survive (Hu et al., 2010).

Similar findings have also resulted from a number of other studies of cooperation in both synthetic and natural microbial systems. For instance, in studies of yeast that secrete sugar-degrading enzymes in a cooperative fashion, the presence of environmental stressors such as low population density of common-good producers (Greig and Travisano, 2004; Sanchez and Gore, 2013; Waite and Shou, 2012), low nutrient concentration (Gore et al., 2009; Waite and Shou, 2012), and competition from other species (Celiker and Gore, 2013), has been shown to increase the benefit to cooperation. Similar trends have also been noted in *Pseudomonas* systems (Brockhurst, 2007; Brockhurst et al., 2007), which use signaling molecules of the type we have modeled here. In wild-type organisms these signaling molecules are frequently used to coordinate the formation of biofilms, which are known to form in response to adverse conditions, including

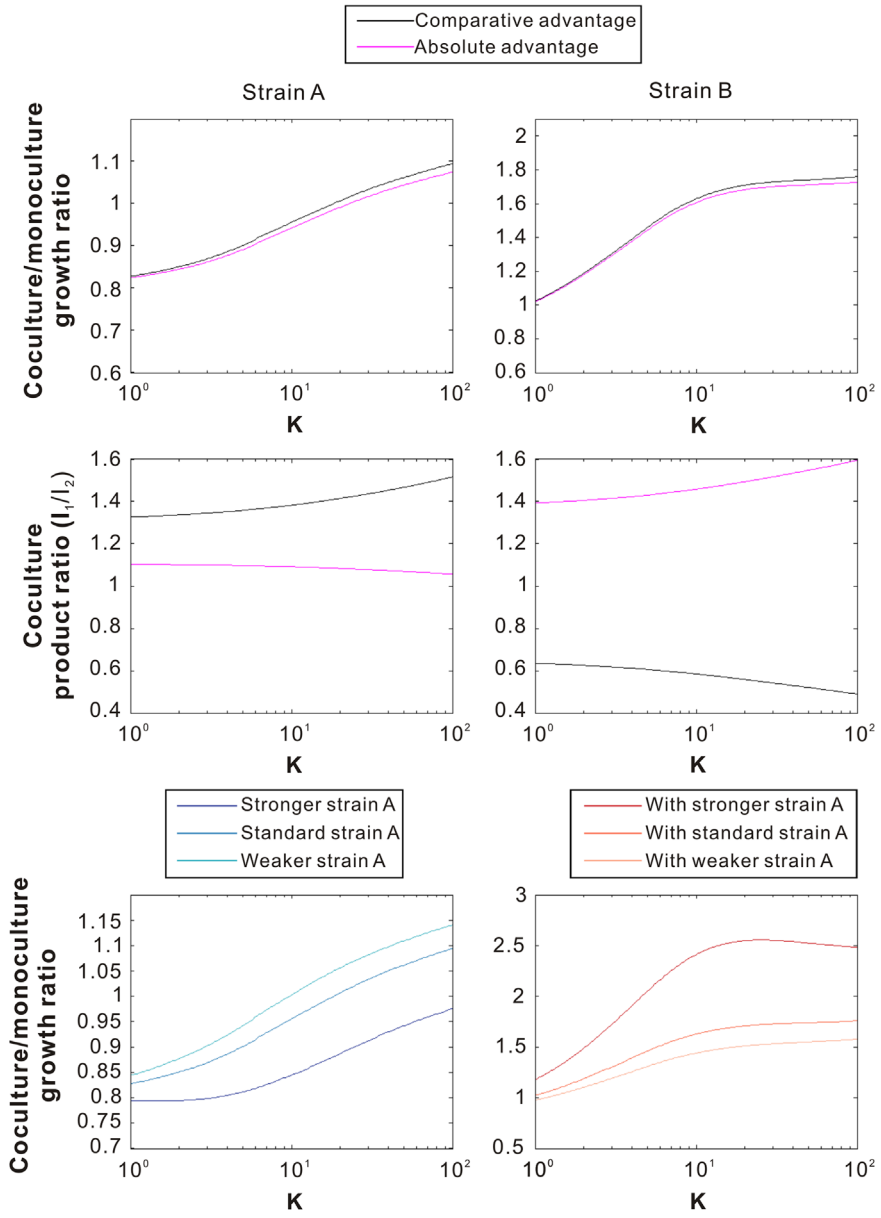

Fig. 10. Alternate efficiency regimes in Conception 2B. In all cases the *x*-axis represents the value of *K*, and the *y*-axis is either coculture/monoculture growth ratio (growth benefit) or the product 1/product 2 production ratio (specialization). Unvaried parameter values are as in Fig. 6 unless otherwise noted. The first and second rows show the difference in effect on growth benefit and specialization, respectively, between the comparative advantage case shown in Figs. 7 and 8 (black lines), and an absolute advantage case that is identical except that the efficiencies for strain B have been switched such that $V_{B1}=1$ and $V_{B2}=0.5$ (magenta lines). The third row shows the effect on growth benefit resulting from changing the efficiency of production of strain A, where the darkest colors represent a case where $V_{A1}=4$ and $V_{A2}=3$ (stronger strain A), the lightest colors represent a case where $V_{A1}=1.5$ and $V_{A2}=1.2$ (weaker strain A), and the intermediate colors represent the case where $V_{A1}=2$ and $V_{A2}=1.5$ (standard strain A) as in Fig. 7.

the presence of antibiotics (Li and Tian, 2012; Mah, 2012). Additionally, a number of microbial systems exist that are normally unicellular but in stringent environments enter into cooperative relationships in which certain individuals sacrifice themselves and/or their ability to reproduce in order to benefit others. Such systems include the yeast *Saccharomyces cerevisiae*, in which older cells undergo programmed cell death and bequeath their nutrients to the younger generation (Fabrizio et al., 2004), as well as the bacterium *Myxococcus xanthus* (Fiegna et al., 2006) and the amoeba *Dictyostelium purpureum* (Mehdiabadi et al., 2006), which form multicellular fruiting bodies in which some cells reproduce and others are relegated exclusively to structural roles.

Given the fact that strain B consistently outgrows strain A in both Conceptions 1 and 2, a question arises as to whether the cooperative interaction could remain stable over many generations, or whether strain A would eventually drop out of the population after being repeatedly outgrown by strain B. The previous work by Chuang et al. (2009) provides some illumination. In the Chuang system, a producer strain makes a signaling molecule that all cells require to express an antibiotic resistance gene, and a non-producer strain merely benefits from the other strain's production. When different cocultures were inoculated using a variety of ratios of the two strains, an interesting result was obtained in that the fraction of non-producers increased in any given culture, but the fraction of producers increased overall when the results from all cultures were summed. This is due to the fact that groups with a higher starting fraction of producers grew more. The case would likely be similar for the strains proposed here, where one strain produces more and the other therefore benefits more.

This leads to the hypothesis that, in the absence of mechanisms for recognizing and directly rewarding strong producers, the cooperative interactions described here could still be stable under conditions of repeated bottlenecks, where multiple groups grow from random assortments of cells at numbers low enough to introduce significant variation in the fractions of the two strains between different groups. After regrowth and mixture, the process is repeated with another set of bottlenecks. The greater relative growth of the progenitor groups that received a larger fraction of the high-producing strain A after bottlenecks would likely favor the maintenance of strain A in the overall population. In addition to the work of Chuang and coworkers, a great deal of effort has been directed at determining the conditions under which bottlenecks and spatial structure can select for cooperation (Bull and Harcombe, 2009; Chao and Levin, 1981; Datta et al., 2013; Hamilton, 1964; Harcombe, 2010; Momeni et al., 2013; Muller et al., 2014; Nowak and May, 1992; Smith, 1964; Waite and Shou, 2012).

Another interesting point to consider is the idea that antibiotics themselves could in some cases act as signals to induce cooperation. Cornforth and Foster (2013) have recently hypothesized that microbes may detect competitors via competition-induced stress, which is supported by the fact that production of antibiotics and toxins is frequently up-regulated by stressors such as nutrient limitation, cell damage, and oxidative stress, which could result from the presence of competitors, but is rarely enhanced by strictly abiotic stressors such as heat-shock and osmotic stress. Additionally, a number of investigators have shown that many antibiotics induce specific transcriptional changes in bacteria at concentrations too low to affect growth, leading some to hypothesize that antibiotics act as signaling molecules in natural environments (Davies, 2006; Fajardo and Martinez, 2008). The types of genes up-regulated depend on the strain and the compound but in a number of cases include genes for biofilm formation and cell adhesion (Davies et al., 2006; Linares et al., 2006), functions obviously associated with intercellular cooperation. Thus it may be the case that, at least in some contexts, microbial antibiotic production plays a dual role of attacking competitors while signaling friendly cells to band together for mutual benefit.

In contrast to the trend of environmental stress encouraging cooperation, making it intrinsically harder for the strains to produce the antibiotic resistance genes typically reduces the benefit to cooperation. Specifically, the V and P parameters, which represent respectively the maximum rate at which product can be turned into growth and the growth penalty for making the products, are likely intrinsic to the system and unlikely to be significantly modulated by changing external conditions such as antibiotic concentration. Changing either of these parameters can be considered as changing the cost of cooperation, and previous work in designed bacteria (Chuang et al., 2010) and yeast (Gore et al., 2009) has shown that increasing the cost of cooperation decreases the benefit gained. The one quasi-exception we noted was in Conception 2, where the higher-producing strain (strain A) benefits more from cooperation at lower V (lower production capacity), which is likely because a lower intrinsic production rate minimizes the opportunity for the lower-producing strain (strain B) to profit from the higher production of strain A without contributing production itself.

A next step would be testing these models *in vivo*, and the results presented here provide useful guidelines and testable hypotheses for designing such experiments. The first step would be to build a base strain that expresses two antibiotic resistance genes in response to two respective signaling molecules. For the signaling molecules, the rhl and lux systems have been reported to be orthogonal (Hu et al., 2010), and methods exist for reducing cross-talk should it occur (Brenner et al., 2007; Smith et al., 2008). Alternatively one or the other of the rhl and lux systems could be used together with an orthogonal peptide signal (Marchand and Collins, 2013). Once the base strains are built, the accuracy of Eqs. (4) and (5) could then be verified by exogenously adding the signaling molecules at different concentrations to examine the effect on growth. Values for V and K could then be estimated. These parameters could also be checked for their dependence on antibiotic concentration.

For Conception 1, the genes for producing the signaling molecules would need to be put under the control of four different exogenous inducers, and then mapping functions for generating a linear response in growth rate from inducer concentrations would need to be experimentally determined. A value for P could also be obtained from these experiments. Equivalents to the heat maps presented here could then be generated by growing the cells in 96-well plates along gradients of inducer concentrations and measuring growth rates directly.

For Conception 2 in particular, the results presented here give a great deal of guidance for how the gene circuits should be designed and tested to maximize the chances of successfully replicating the effects of comparative advantage. Specifically, better performance should be seen under Conception 2B, with relatively weak promoters for the antibiotic resistance genes (lower V), with relatively narrow differences in efficiencies of production between the two strains, and at higher antibiotic concentrations (higher K). More detailed simulations of transcription, translation, enzyme catalysis, and export could also be developed as necessary to guide the design of both Conceptions 1 and 2.

Besides expanding the demonstrated reach of the comparative advantage theory and proving that bacteria are in principle capable of implementing and benefitting from such trading relationships, the implementation of such systems *in vivo* would also expand our toolkit for engineering bacterial consortia to efficiently execute human-directed tasks (Shong et al., 2012). As a hypothetical example, in a consortium of two microbes that can both produce a desired product but have differing efficiencies in performing different steps of the relevant metabolic pathway, if the microbes are designed to allow trading of intermediates, responsive signaling networks such as those modeled in Conception 2 herein could be used to maximize overall production and to continuously adapt to changes in environmental variables, such as the concentrations of intermediates, products, and other cells. The results presented herein represent a theoretical proof of this principle.

Finally, it is possible and perhaps likely that wild-type microbes enter into comparative-advantage-like social interactions in natural settings. In order to find such interactions, a series of pair-wise coculture growth experiments could be performed, and the results compared to the monoculture case, as was reported, for instance, by Foster and Bell (2012). Those strains that grew better together than separately are candidates for natural examples of microbial comparative advantage, and this could potentially be confirmed by expression studies comparing gene regulation in monoculture and coculture, and/or mutagenesis studies to determine the genes required for mutualism. It is also possible that comparative advantage might be more likely to come into play in tandem with kin selection. Comparative advantage could potentially arise even between genetically identical cells if they are subjected to different environments, such as the center versus the edge of a colony or biofilm. Expression studies examining the differences between cells in different locations in a biofilm (Lenz et al., 2008) could potentially turn up such examples. It may be that comparative advantage is universally applied in all domains of life.

Author contributions

P.J.E. and Z.B.S. conceived the project. P.J.E. devised the mathematical models, produced the data, and wrote the manuscript.

All authors participated in analyzing and interpreting the data and in editing and revising the manuscript.

Conflict of interest

The authors declare no conflict of interest.

Acknowledgements

We thank Xi Chen, Jonathan Dingwell, Marvin Whiteley, and Daniel Cornforth for helpful discussions. This material is based upon work supported in part by the National Science Foundation Graduate Research Fellowship under Grant no. DGE-1110007, the Welch Foundation (F-1654), and a National Security Science and Engineering Faculty Fellowship (FA9550-10-1-0169)

Appendix A. Supporting information

Supplementary data associated with this article can be found in the online version at http://dx.doi.org/10.1016/j.jtbi.2014.09.030.

References

Axelrod, R., Hamilton, W.D., 1981. The evolution of cooperation. Science 211, 1390–1396.
Balagadde, F.K., Song, H., Ozaki, J., Collins, C.H., Barnet, M., Arnold, F.H., Quake, S.R., You, L., 2008. A synthetic *Escherichia coli* predator-prey ecosystem. Mol. Syst. Biol. 4, 187.
Biliouris, K., Babson, D., Schmidt-Dannert, C., Kaznessis, Y.N., 2012. Stochastic simulations of a synthetic bacteria-yeast ecosystem. BMC Syst. Biol. 6, 58.
Brenner, K., Karig, D.K., Weiss, R., Arnold, F.H., 2007. Engineered bidirectional communication mediates a consensus in a microbial biofilm consortium. Proc. Natl. Acad. Sci. U.S.A. 104, 17300–17304.
Brockhurst, M.A., 2007. Population bottlenecks promote cooperation in bacterial biofilms. PLoS One 2, e634.
Brockhurst, M.A., Buckling, A., Gardner, A., 2007. Cooperation peaks at intermediate disturbance. Curr. Biol. 17, 761–765.
Bull, J.J., Harcombe, W.R., 2009. Population dynamics constrain the cooperative evolution of cross-feeding. PLoS One 4, e4115.
Celiker, H., Gore, J., 2013. Cellular cooperation: insights from microbes. Trends Cell Biol. 23, 9–15.
Chao, L., Levin, B.R., 1981. Structured habitats and the evolution of anticompetitor toxins in bacteria. Proc. Natl. Acad. Sci. U.S.A. 78, 6324–6328.
Chuang, J.S., Rivoire, O., Leibler, S., 2009. Simpson's paradox in a synthetic microbial system. Science 323, 272–275.
Chuang, J.S., Rivoire, O., Leibler, S., 2010. Cooperation and Hamilton's rule in a simple synthetic microbial system. Mol. Syst. Biol. 6, 398.
Cornforth, D.M., Foster, K.R., 2013. Competition sensing: the social side of bacterial stress responses. Nat. Rev. Microbiol. 11, 285–293.
Craig Maclean, R., Brandon, C., 2008. Stable public goods cooperation and dynamic social interactions in yeast. J. Evol. Biol. 21, 1836–1843.
Crespi, B.J., 2001. The evolution of social behavior in microorganisms. Trends Ecol. Evol. 16, 178–183.
Danino, T., Mondragon-Palomino, O., Tsimring, L., Hasty, J., 2010. A synchronized quorum of genetic clocks. Nature 463, 326–330.
Datta, M.S., Korolev, K.S., Cvijovic, I., Dudley, C., Gore, J., 2013. Range expansion promotes cooperation in an experimental microbial metapopulation. Proc. Natl. Acad. Sci. U.S.A. 110, 7354–7359.
Davies, J., 2006. Are antibiotics naturally antibiotics? J. Ind. Microbiol. Biotechnol. 33, 496–499.
Davies, J., Spiegelman, G.B., Yim, G., 2006. The world of subinhibitory antibiotic concentrations. Curr. Opin. Microbiol. 9, 445–453.
Diggle, S.P., Griffin, A.S., Campbell, G.S., West, S.A., 2007. Cooperation and conflict in quorum-sensing bacterial populations. Nature 450, 411–414.
Duarte, A., Weissing, F.J., Pen, I., Keller, L., 2011. An evolutionary perspective on self-organized division of labor in social insects. Annu. Rev. Ecol. Evol. Syst. Vol 42 (42), 91–110.
Dunham, M.J., 2007. Synthetic ecology: a model system for cooperation. Proc. Natl. Acad. Sci. U.S.A. 104, 1741–1742.
Elowitz, M.B., Leibler, S., 2000. A synthetic oscillatory network of transcriptional regulators. Nature 403, 335–338.
Fabrizio, P., Battistella, L., Vardavas, R., Gattazzo, C., Liou, L.L., Diaspro, A., Dossen, J. W., Gralla, E.B., Longo, V.D., 2004. Superoxide is a mediator of an altruistic aging program in *Saccharomyces cerevisiae*. J. Cell Biol. 166, 1055–1067.
Fajardo, A., Martinez, J.L., 2008. Antibiotics as signals that trigger specific bacterial responses. Curr. Opin. Microbiol. 11, 161–167.
Fiegna, F., Yu, Y.T., Kadam, S.V., Velicer, G.J., 2006. Evolution of an obligate social cheater to a superior cooperator. Nature 441, 310–314.
Fletcher, J.A., Doebeli, M., 2009. A simple and general explanation for the evolution of altruism. Proc. R. Soc. B. 276, 13–19.
Foster, K.R., Bell, T., 2012. Competition, not cooperation, dominates interactions among culturable microbial species. Curr. Biol. 22, 1845–1850.
Gardner, A., West, S.A., Wild, G., 2011. The genetical theory of kin selection. J. Evol. Biol. 24, 1020–1043.
Gardner, T.S., Cantor, C.R., Collins, J.J., 2000. Construction of a genetic toggle switch in *Escherichia coli*. Nature 403, 339–342.
Gavrilets, S., 2010. Rapid transition towards the division of labor via evolution of developmental plasticity. PLoS Comput. Biol. 6, e1000805.
Gore, J., Youk, H., van Oudenaarden, A., 2009. Snowdrift game dynamics and facultative cheating in yeast. Nature 459, 253–256.
Greig, D., Travisano, M., 2004. The Prisoner's Dilemma and polymorphism in yeast SUC genes. Proc. R. Soc. B. 271 (Suppl 3), S25–S26.
Griffin, A.S., West, S.A., Buckling, A., 2004. Cooperation and competition in pathogenic bacteria. Nature 430, 1024–1027.
Hamilton, W.D., 1963. Evolution of altruistic behavior. Am. Nat. 97 (354-&).
Hamilton, W.D., 1964. The genetical evolution of social behaviour. I&II. J. Theor. Biol. 7, 1–52.
Harcombe, W., 2010. Novel cooperation experimentally evolved between species. Evolution 64, 2166–2172.
Hu, B., Du, J., Zou, R.Y., Yuan, Y.J., 2010. An environment-sensitive synthetic microbial ecosystem. PLoS One 5, e10619.
Isaacs, F.J., Dwyer, D.J., Ding, C., Pervouchine, D.D., Cantor, C.R., Collins, J.J., 2004. Engineered riboregulators enable post-transcriptional control of gene expression. Nat. Biotechnol. 22, 841–847.
Kerner, A., Park, J., Williams, A., Lin, X.N., 2012. A programmable *Escherichia coli* consortium via tunable symbiosis. PLoS One 7, e34032.
Kubo, I., Hosoda, K., Suzuki, S., Yamamoto, K., Kihara, K., Mori, K., Yomo, T., 2013. Construction of bacteria-eukaryote synthetic mutualism. Biosystems 113, 66–71.
Kummerli, R., Gardner, A., West, S.A., Griffin, A.S., 2009. Limited dispersal, budding dispersal, and cooperation: an experimental study. Evolution 63, 939–949.
Lehninger, A.L., Nelson, D.L., Cox, M.M., 2013. Lehninger Principles of Biochemistry. W.H. Freeman, New York, NY.
Lenz, A.P., Williamson, K.S., Pitts, B., Stewart, P.S., Franklin, M.J., 2008. Localized gene expression in *Pseudomonas aeruginosa* biofilms. Appl. Environ. Microbiol. 74, 4463–4471.
Li, Y.H., Tian, X., 2012. Quorum sensing and bacterial social interactions in biofilms. Sensors (Basel) 12, 2519–2538.
Linares, J.F., Gustafsson, I., Baquero, F., Martinez, J.L., 2006. Antibiotics as intermicrobial signaling agents instead of weapons. Proc. Natl. Acad. Sci. U.S.A. 103, 19484–19489.
Lucks, J.B., Qi, L., Mutalik, V.K., Wang, D., Arkin, A.P., 2011. Versatile RNA-sensing transcriptional regulators for engineering genetic networks. Proc. Natl. Acad. Sci. U.S.A. 108, 8617–8622.
Mah, T.F., 2012. Biofilm-specific antibiotic resistance. Future Microbiol. 7, 1061–1072.
Marchand, N., Collins, C.H., 2013. Peptide-based communication system enables *Escherichia coli* to *Bacillus megaterium* interspecies signaling. Biotechnol. Bioeng. 110, 3003–3012.
Maynard Smith, J., Szathmáry, E., 1995. The Major Transitions in Evolution. W.H. Freeman Spektrum, Oxford; New York.
Mehdiabadi, N.J., Jack, C.N., Farnham, T.T., Platt, T.G., Kalla, S.E., Shaulsky, G., Queller, D.C., Strassmann, J.E., 2006. Social evolution: kin preference in a social microbe. Nature 442, 881–882.
Momeni, B., Waite, A.J., Shou, W., 2013. Spatial self-organization favors heterotypic cooperation over cheating. Elife 2, e00960.
Mondragon-Palomino, O., Danino, T., Selimkhanov, J., Tsimring, L., Hasty, J., 2011. Entrainment of a population of synthetic genetic oscillators. Science 333, 1315–1319.
Monod, J., 1942. Recherches sur la croissance des cultures bactériennes. Hermann & Cie, Paris.
Monod, J., 1949. The growth of bacterial cultures. Annu. Rev. Microbiol. 3, 371–394.
Muller, M.J., Neugeboren, B.I., Nelson, D.R., Murray, A.W., 2014. Genetic drift opposes mutualism during spatial population expansion. Proc. Natl. Acad. Sci. U.S.A. 111, 1037–1042.
Muro-Pastor, A.M., Hess, W.R., 2012. Heterocyst differentiation: from single mutants to global approaches. Trends Microbiol. 20, 548–557.
Na, D., Yoo, S.M., Chung, H., Park, H., Park, J.H., Lee, S.Y., 2013. Metabolic engineering of *Escherichia coli* using synthetic small regulatory RNAs. Nat. Biotechnol. 31, 170–174.
Nahum, J.R., Harding, B.N., Kerr, B., 2011. Evolution of restraint in a structured rock-paper-scissors community. Proc. Natl. Acad. Sci. U.S.A. 108 (Suppl. 2), 10831–10838.
Nowak, M.A., May, R.M., 1992. Evolutionary games and spatial chaos. Nature 359, 826–829.
Page Jr., R.E., Erber, J., 2002. Levels of behavioral organization and the evolution of division of labor. Naturwissenschaften 89, 91–106.
Raihani, N.J., Bshary, R., 2011. Resolving the iterated prisoner's dilemma: theory and reality. J. Evol. Biol. 24, 1628–1639.
Rainey, P.B., Rainey, K., 2003. Evolution of cooperation and conflict in experimental bacterial populations. Nature 425, 72–74.

Ricardo, D., 1817. On the Principles of Political Economy and Taxation. J. Murray, London.
Rumbaugh, K.P., Diggle, S.P., Watters, C.M., Ross-Gillespie, A., Griffin, A.S., West, S.A., 2009. Quorum sensing and the social evolution of bacterial virulence. Curr. Biol. 19, 341–345.
Saito, H., Inoue, T., 2009. Synthetic biology with RNA motifs. Int. J. Biochem. Cell Biol. 41, 398–404.
Sanchez, A., Gore, J., 2013. Feedback between population and evolutionary dynamics determines the fate of social microbial populations. PLoS Biol. 11, e1001547.
Shapiro, J.A., 1998. Thinking about bacterial populations as multicellular organisms. Annu. Rev. Microbiol. 52, 81–104.
Shendure, J., Porreca, G.J., Reppas, N.B., Lin, X., McCutcheon, J.P., Rosenbaum, A.M., Wang, M.D., Zhang, K., Mitra, R.D., Church, G.M., 2005. Accurate multiplex polony sequencing of an evolved bacterial genome. Science 309, 1728–1732.
Shong, J., Jimenez Diaz, M.R., Collins, C.H., 2012. Towards synthetic microbial consortia for bioprocessing. Curr. Opin. Biotechnol. 23, 798–802.
Shou, W., Ram, S., Vilar, J.M., 2007. Synthetic cooperation in engineered yeast populations. Proc. Natl. Acad. Sci. U.S.A. 104, 1877–1882.
Smith, C., Song, H., You, L., 2008. Signal discrimination by differential regulation of protein stability in quorum sensing. J. Mol. Biol. 382, 1290–1297.
Smith, J.M., 1964. Group selection and kin selection. Nature 201, 1145–1147.
Tanouchi, Y., Pai, A., Buchler, N.E., You, L., 2012. Programming stress-induced altruistic death in engineered bacteria. Mol. Syst. Biol. 8, 626.
Torrens, R., 1815. An essay on the External Corn Trade. Printed for J. Hatchard, London.
Waite, A.J., Shou, W., 2012. Adaptation to a new environment allows cooperators to purge cheaters stochastically. Proc. Natl. Acad. Sci. U.S.A. 109, 19079–19086.
Wilson, D.S., Wilson, E.O., 2007. Rethinking the theoretical foundation of socio-biology. Q. Rev. Biol. 82, 327–348.
Wintermute, E.H., Silver, P.A., 2010. Emergent cooperation in microbial metabolism. Mol. Syst. Biol. 6, 407.